ENVISAT GOMOS report: February 2007

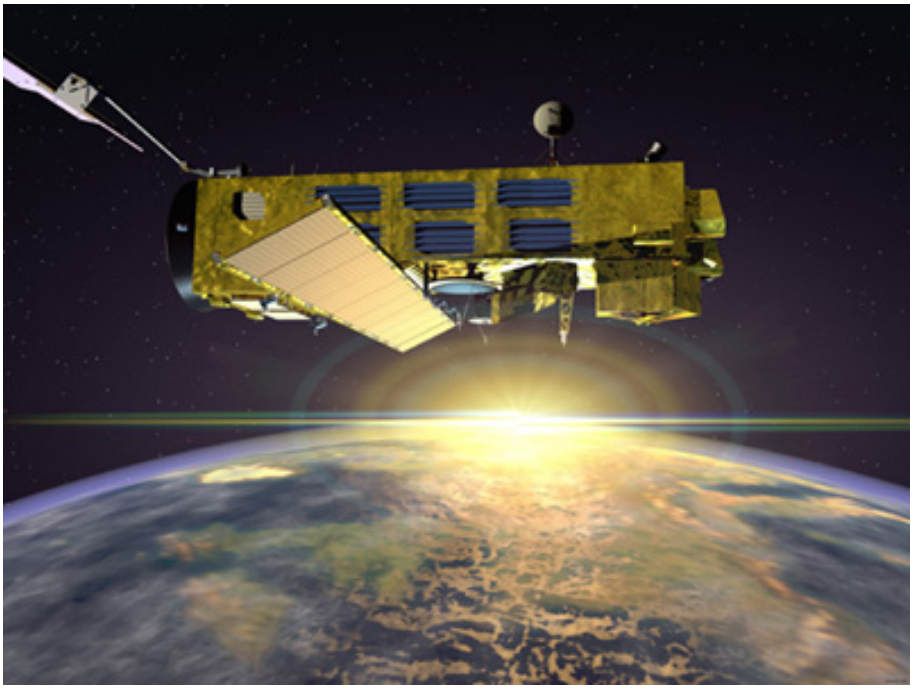

Prepared by:	Daniele Del Cavallo, Fabrizio Niro – SERCO
Approved by:	Gilbert Barrot – ACRI
Inputs from:	GOMOS Quality Working Group, ECMWF

Issue:	1.0
Reference:	ENVI-SPPA-EOPG-TN-07-0016
Date of issue:	15nd March 2007
Status:	Reviewed
Document type:	Technical Note

TABLE OF CONTENTS

1 INTRODUCTION

The GOMOS monthly report documents the current status and recent changes to the GOMOS instrument, its data processing chain, and its data products.
The Monthly Report (hereafter MR) is composed of analysis results obtained by the Data Processing and Quality Control, combined with inputs received from the different entities working on GOMOS operation, calibration, product validation and data quality. These teams participate in the GOMOS Quality Working Group:

- European Space Agency (ESRIN, ESOC, ESTEC-PLSO)
- DPQC
- ACRI
- Service d'Aeronomie
- Finnish Meteorological Institute
- IASB-Belgian Institute for Space Aeronomy
- Astrium Space
- ECMWF

In addition, the group interfaces with the Atmospheric Chemistry Validation Team.

1.1 Scope

The main objective of the Monthly Report is to give, on a regular basis, the status of GOMOS instrument performance, data acquisition, results of anomaly investigations, calibration activities and validation campaigns. The following six sections compose the MR:

- Summary
- Unavailability
- Instrument Configuration and Performance
- Level 1 Product Quality Monitoring
- Level 2 Product Quality Monitoring
- Validation Activities and Results

1.2 References

[1] ENVISAT Weekly Mission Operations Report #236, 237#, #238, #239
[2] ECMWF GOMOS Monthly Reports

1.3 Acronyms and Abbreviations

ACVT	Atmospheric Chemistry Validation Team
ADC	Analogue-to-Digital Converter
ADF	Auxiliary Data File

ADS	Auxiliary Data Server
ANX	Ascending Node Crossing
AOCS	Attitude and Orbit Control System
ARB	Anomaly Review Board
ARF	Archiving Facility (PDS)
CCU	Central Communication Unit
CFS	CCU Flight Software
CNES	Centre National d'Études Spatiales
CTI	Configuration Table Interface / Configurable Transfer Item
CR	Cyclic Report
DC	Dark Charge
DMOP	Detailed Mission Operation Plan
DPM	Detailed Processing Model
DPQC	Data Processing and Quality Control
DS	Data Server
DSA	Dark Sky Area
DSD	Data Set Descriptor
ECMWF	European Centre for Medium Weather Forecast\
EO	Earth Observation
EQSOL	Equipment Switch Off Line
ESA	European Space Agency
ESL	Expert Support Laboratory
ESRIN	European Space Research Institute
ESTEC	European Space Research & Technology Centre
ESOC	European Space Operations Centre
FCM	Fine Control Mode
FinCoPAC	Finnish Products Archiving Center
FMI	Finnish Meteorological Institute
FOCC	Flight Operations Control Centre (ENVISAT)
FP1	Fast Photometer 1
FP2	Fast Photometer 2
GADS	Global Annotations Data Set
GOMOS	Global Ozone Monitoring by Occultation of Stars
GOPR	Gomos Prototype
GS	Ground Segment
HK	Housekeeping
IASB	Institut d'Aeronomie Spatiale de Belgique
IAT	Interactive Analysis Tool
ICU	Instrument Control Unit
IDL	Interactive Data Language
IECF	Instrument Engineering and Calibration Facilities
IMK	Institute of Meteorology Karlsruhe (Meteorologisch Institut Karlsuhe)
INV	Inventory Facilities (PDS)
IPF	Instrument Processing Facilities (PDS)
JPL	Jet Propulsion Laboratory
LAN	Local Area Network
LMA	Levenberg-Marquardt Algorithm
LPCE	Laboratoire de Physique et Chimie de l'Environnement

LRAC	Low Rate Archiving Center
LUT	Look Up Table
MCMD	Macro Command
MDE	Mechanism Drive Electronics
MIP	Most Illuminated Pixel
MPH	Main Product Header
MPS	Mission Planning System
MR	Monthly Report
NRT	Near Real Time
OBDH	On-Board Data Handling
OBT	On Board Time
OCM	Orbit Control Manoeuvre
OOP	Out-of-plane
OP	Operational Phase of ENVISAT
PAC	Processing and Archiving Centre (PDS)
PCF	Product Control Facility
PDCC	Payload Data Control Centre (PDS)
PDHS	Payload Data Handling Station (PDS)
PDHS-E	Payload Data Handling Station – ESRIN
PDHS-K	Payload Data Handling Station – Kiruna
PDS	Payload Data Segment
PEB	Payload Equipment Bay
PLSOL	Payload Switch off Line
PMC	Payload Module Computer
PRNU	Pixel Response Non Uniformity
PSO	On-Orbit Position
QC	Quality Control
QUARC	Quality Analysis and Reporting Computer
QWG	Quality Working Group
RDV	RenDez-Vous
RGT	ROP Generation Tool
RIVM	Rijksinstituut voor Volksgezondheid en Milieu
ROP	Reference Operations Plan
RRM	Rate Reduction Mode
RTS	Random Telegraphic Signal
SA	Service d'Aeronomie
SAA	South Atlantic Anomaly
SATU	Star Acquisition and Tracking Unit
SFA	Steering Front Assembly
SFCM	Stellar Fine Control Mode
SFM	Steering Front Mechanism
SM	Service Module
SMNA	Servicio Meteorológico Nacional de Argentina
SODAP	Switch On and Data Acquisition Phase
SPA1	Spectrometer A CCD 1
SPA2	Spectrometer A CCD 2
SPB1	Spectrometer B CCD 1
SPB2	Spectrometer B CCD 2

SPH	Specific Product Header
SQADS	Summary Quality Annotation Data Set
SSP	Sun Shade Position
SYSM	Stellar Yaw Steering Mode
SZA	Solar Zenith Angle
VCCS	Voice Coil Command Saturation

2 SUMMARY

Instrument availability (section 3.1): GOMOS was switched to Reset/Wait on 1st February due to a MCMD Transfer Acknowledge Error. This anomaly already occurred in 2003 (ref. AR-ENV-744). After a complete memory dump, GOMOS was recovered successfully and resumed operations on 2nd February at 19:34:23 UTC.

Instrument operations (section 4.1.2): Since December 17th the starting altitude is set back to its nominal value (130km), this value shall not be changed for the rest of the mission because it impacts significantly L2 products quality.

Data availability when instrument was in operation (section 3.4): During the reporting month an anomaly was detected in the computation of the GOMOS L0 and L1 NRT products statistics, therefore the statistics are not updated and will be reported in the next MR.

Data availability for users (section 3.5): Routine dissemination of Level 1b and Level 2 products produced by the PDS to the users is enabled. Level 1b data are available on request to the EO Helpdesk (EOHelp@esa.int), while level 2 data are available for the whole mission on different ftp sites. **Be aware that the GOMOS level 2 products from ESRIN** are available now in a new ftp server while the old one has been dismissed (see section 3.5 for detailed information). All data (reprocessed, NRT and consolidated) are processed with the same version of GOMOS processor.

Pointing performance (section 4.6.1): the SATU NEA ("Y" axis) has a gradual increase since mid April 2006. This increase is due to fluctuations of the SATU 'Y' data observed at the beginning of the occultations (starting at 130 km that corresponds to an elevation angle of around 65°). Preliminary investigations carried out by the ESL, ESA and industry point to a problem on the SFM (mechanical or electrical) and not to a problem on the SATU itself. Since mid June the increase was stable for a while at around 5.5 micro radians. Currently the SATU NEA is stable at around 2.2 micro radians and the start altitude of the occultations is 130 Km.

Temperatures (section 4.3): The CCD temperatures show the expected global increase due to the radiator ageing. Another expected variation of the temperatures, the seasonal one, with amplitude of around 0.8 degree can also be observed.

Modulation signal (section 4.5.2): The standard deviation of the modulation signal shows high values during summer time for the ESRIN data, it now being confirmed that the South Atlantic Anomaly is the cause of these unexpected peaks. The quality of ESRIN data, in particular over the SAA zone, is impacted but the measure of this impact is under investigation. However, in the second half of the months of October (2004, 2005 and 2006) the peaks are smaller because the DSA zone where the data are taken for this analysis is moving towards the Northern Hemisphere. At the end of October the DSA zone is

definitely chosen by the planning system in the Northern Hemisphere (to fill the criteria 'DSA in full dark limb conditions') and the high peaks disappear.

Star detection performance (section 4.6.3): the stars should be detected not far from the SATU center, that is, pixel number 145 in elevation and number 205 in azimuth. It has been observed that the azimuth MIP was within the threshold since September 2002 until the occurrence of the VCCS anomaly on January 2005. The reason for the change in trend observed after the anomaly is, at the moment, not understood. The elevation MIP had a significant variation until 12th December 2003 when a new PSO algorithm was activated in order to reduce the deviations of the ENVISAT platform attitude with respect to the nominal one. Similarly to the azimuth, after the anomaly of January 2005 the Elevation MIP has a drift that has no explanation. Investigations are ongoing to try to understand this behavior of the MIP as although it does not impact the data quality, it may invalidate attitude monitoring by GOMOS and could represent a hidden anomaly.

Radiometric sensitivity monitoring (section 5.4.1): for stars 25 and 9, the UV ratio is greater than the threshold 10%. It is clear that there is a global decrease of UV ratios for all the stars. This confirms the expected degradation suffered by the UV optics that is, anyway, very small considering also the small variation for the rest of the stars. For the photometers radiometric sensitivity ratios it is observed that every star has a variation that seems to be seasonally related. The variation is significant for stars 25 and 18. After some investigations performed by the QWG that exclude an inaccurate reflectivity correction LUT, it seems that the PH1/2 radiometric sensitivity variations could come from the fact that the spectrometers and the photometers are not illuminated the same way when the straylight appears.

Auxiliary Data File (sections 5.1.2): Three GOM_CAL_AX with updated DC maps have been disseminated during the reporting month.

3 INSTRUMENT AND DATA AVAILABILITY

3.1 GOMOS Unavailability Periods

On table 3.1-1 there is a list of GOMOS unavailability reports issued during the period 1st January to 31t January 2007.

GOMOS was switched to Reset/Wait on 1st February due to a MCMD Transfer Acknowledge Error. This anomaly already occurred in 2003 (ref. AR-ENV-744). After a complete memory dump, GOMOS was recovered successfully and resumed operations on 2nd February at 19:34:23 UTC.

Table 3.1-1: List of unavailability periods issued during the reporting period

Reference of unavailability report	Start time Star orbit	Stop time Stop orbit	Description
EN-UNA-2007/0028	01 Feb 2007 23:26:30.000 Day of Year = 032 Orbit = 25750	02 Feb 2007 19:34:23.000 Day of Year = 033 Orbit =25762	GOMOS in ICU RS/WT/INI (Unplanned)

3.2 Stars Lost in Centering

The acquisition of a star initiates with a rallying phase where the telescope mechanism is directed towards the expected position of the star. Subsequently the acquisition procedure enters into detection mode, where the SATU star tracker output signal is pre-processed for spot presence survey and for the location of the most illuminated couple of adjacent pixels for two added lines, over the detection field. The Most Illuminated Pixel (MIP) defines the position of the first SATU centering window. The following step in the acquisition sequence is then initiated and consists of a centering phase where the SATU output signal is pre-processed for spot presence survey over the maximum of 10x10 pixel field. This allows the third phase to begin: the tracking phase.

The centering phase has occasionally resulted in loss of the star from the field of view. Fig. 3.2-1 reports the percentage of the stars lost in centering for the period 03-FEB-2003 to 04-MAR-2007. It can be seen that only three stars, mainly weak stars (higher star id means higher magnitude) are lost during the centering phase between 4 and 7 % of their planned observations. The star id 115 was lost almost 9% of the times but it was planned to be occulted twenty three times and was lost twice (in period 19-25 January 2004), so this percentage of loss is not statistically significant.

As the monitoring shows neither a trend nor excessively high percentages of loss, there is no need for the moment to reject any star from the catalogue, and there is no indication of instrument-related problems.

Now with the instrument in a new operation scenario, the stars are also lost due to the anomaly “elevation voice coil command saturation” even if the instrument is not going anymore to Stand by / Refuse mode (section 3.3).

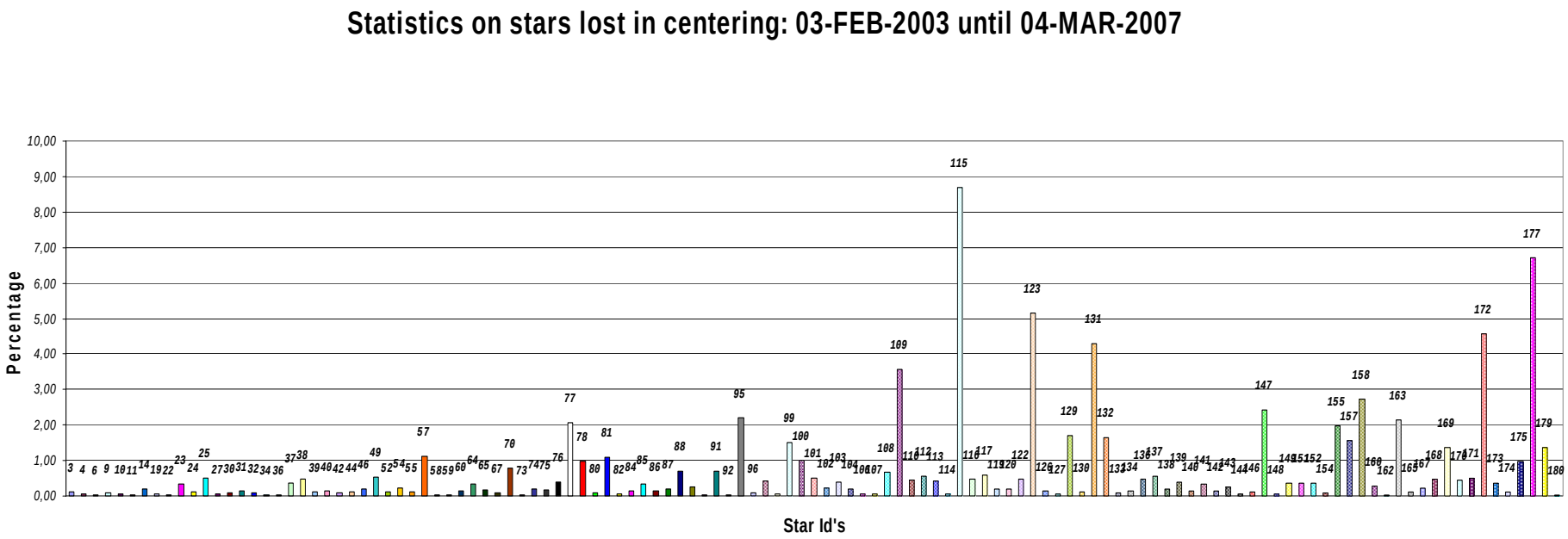

Figure 3.2-1: Statistics on stars that have been lost during the centering phase. The number above the columns correspond to the Star ID

3.3 Stars lost due to VCCS anomaly

No VCCS anomalies occurred during the reporting period

3.4 Data Generation Gaps

The trend in percentage of available NRT data within the archives PDHS-K and PDHS-E is depicted in fig. 3.4-1 (when instrument was in operation). It is a good indicator on how the PDS chain is working in terms of generation and dissemination of data to the archives. The percentage is calculated once per week.

During the reporting month an anomaly was detected in the computation of the GOMOS L0 and L1 NRT products statistics, therefore the statistics are not updated and will be reported in the next MR.

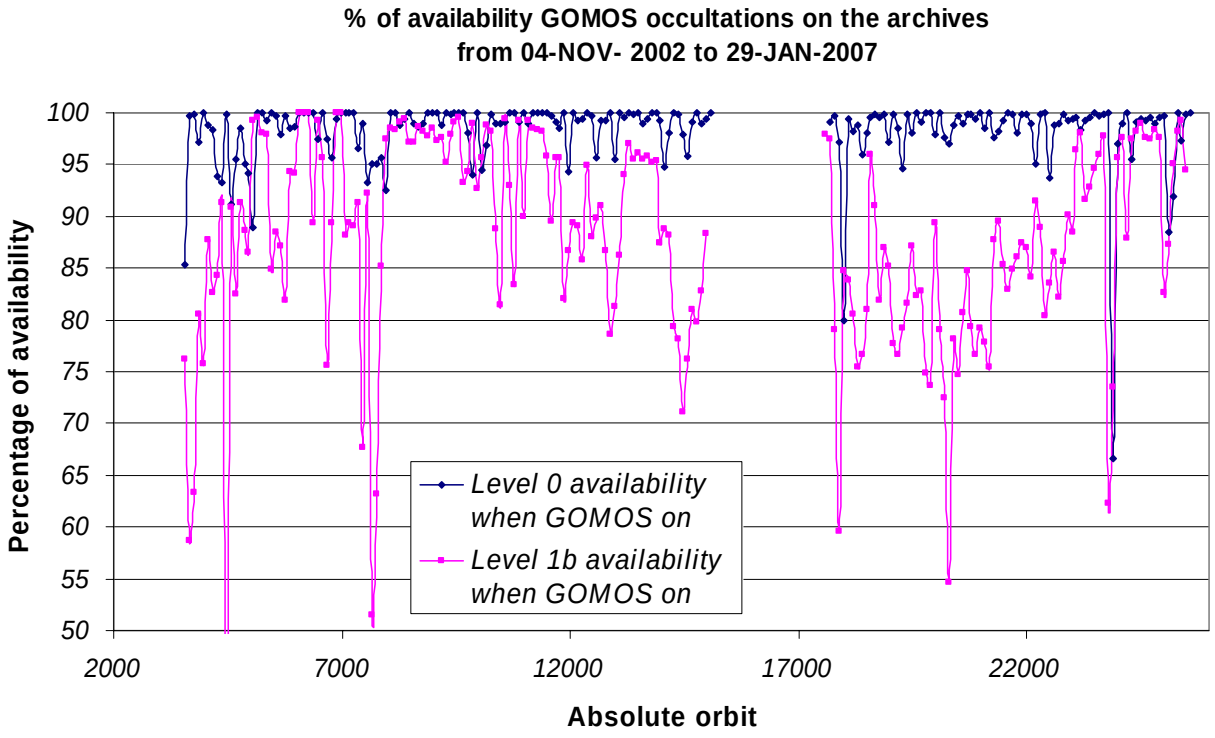

Figure 3.4-1: Percentage of level 0 and level 1b data availability on the archives PDHS-E and PDHS-K

Occultations planned to be acquired but for which no GOM_NL__0P data product has become available are presented in fig. 3.4-2 for the reporting period.

.

[This figure is not reported because an anomaly was detected during the computation of the GOMOS L0 products statistic]

Figure 3.4-2: The pink lines are the orbit segments corresponding to planned data acquisitions for which no GOMOS level 0 product has become available

3.5 Data availability to users

Routine dissemination of higher-level products produced by the PDS to the users is enabled. Level 1b data are available on request to the EO Helpdesk (EOHelp@esa.int), while level 2 data are available for the whole mission. For information on the passwords, please, contact the EO Helpdesk (EOHelp@esa.int):

- Reprocessed products GOM_NL__2P are available at D-PAC ftp server:
  ftp://gomo2usr@ftp-ops.de.envisat.esa.int from **August 2002 to 4th July 2006**.
- Near Real Time products GOM_NL__2P (generated three hours after sensing time) are available on the following servers:
  ftp://gomosusr@oa-es.eo.esa.int (note the **new server** for ESRIN data)
  ftp://gomosusr@oa-ks.eo.esa.int (for KIRUNA data). **A seven-day rolling archive has been set-up on this server**.
- Consolidated products GOM_NL__2P (generated three weeks after sensing time) are available at D-PAC ftp server
  ftp://gomo2usr@ftp-ops.de.envisat.esa.int **since 23 July 2006**

All data (reprocessed, NRT and consolidated) are processed with the same version of GOMOS processor.

4 INSTRUMENT CONFIGURATION AND PERFORMANCE

4.1 Instrument Operation and Configuration

4.1.1 OPERATIONS SINCE BEGINNING OF MISSION

During the period end of March 2003 to July 2003 the azimuth range had to be decreased in steps (table 4.1-1) to avoid an instrument problem ("Voice_coil_command_saturation" anomaly) that caused GOMOS to go into STAND BY/REFUSE mode. On July 2003 the driver assembly was switched to the redundant B-side and since that date the full azimuth range (-10.8, +90.8) was again available until the second major anomaly occurred on 25th January 2005. Between this date and until the instrument was declared operational again (29th August 2005), GOMOS has been operated for testing and anomaly investigation purposes in different operations scenarios. The changes in azimuth configuration during the whole mission until end of reporting period are summarized in table 4.1-1.

Table 4.1-1: Historical changes in Azimuth configuration when GOMOS is in operations

Date	Orbit	Minimum Azimuth (°)	Maximum Azimuth (°)	Comment
01-MAR-2002		-10.8	+90.8	Nominal
29-MAR-2003 17:40	5635	0.0	+90.8	Reduced
31-MAY-2003 06:22	6530	+4.0	+90.8	Reduced
16-JUN-2003 16:17	6765	+12.0	+90.8	Reduced
15-JUL-2003 01:39	7200	-10.8	+90.8	Nominal
25-JAN-2005 23:33	15200	tests	tests	Different configuration for testing purposes
29-AUG-2005 02:52	18280	-10	+10	Reduced
26-SEP-2005 01:32	18680	-5	+20	Reduced
03-OCT-2005 01:12	18780	-5	+15	Reduced
09-OCT-2005 21:30	18878	-5	+20	Reduced
12-MAR-2006 17:29	21080	+10	+35	Reduced
09-APR-2006 12:47	21480	+5	+30	Reduced
16-APR-2006 15:48	21580	0	+25	Reduced
30-APR-2006 15:08	21780	-5	+20	Reduced
07-MAY-2006 14:48	21880	0	+25	Reduced
14-MAY-2006 14:28	21980	+15	+40	Reduced
28-MAY-2006 13:47	22180	+20	+45	Reduced
04-JUN-2006 13:27	22280	+15	+40	Reduced
18-JUN-2006 12:47	22480	+20	+45	Reduced
25-JUN-2006 12:27	22580	0	+25	Reduced
02-JUL-2006 12:07	22680	-5	+20	Reduced
16-JUL-2006 11:27	22880	0	+25	Reduced
23-JUL-2006 11:07	22980	+10	+35	Reduced
06-AUG-2006 10:26	23180	0	+25	Reduced
27-AUG-2006 09:26	23480	+5	+30	Reduced
03-SEP-2006 09:06	23580	0	+25	Reduced
10-SEP-2006 08:46	23680	-5	+20	Reduced
01-OCT-2006 07:45	23980	+5	+30	Reduced
15-OCT-2006 07:05	24180	-5	+20	Reduced
22-OCT-2006 06:45	24280	0	+25	Reduced
29-OCT-2006 06:25	24380	-5	+20	Reduced

4.1.2 CURRENT OPERATIONS AND CONFIGURATION

The start altitude of the occultations was reduced to 112.5 km for some periods of the GOMOS mission in order to avoid the SATU "Y" axis oscillations (table 4.1-2). After GOMOS ARB of November 2006 it was decided to set the starting altitude back to 130km, in fact this decision is not affecting instrument safety, while it guarantees the expected L2 products quality. Since December 17th the starting altitude is set back to its nominal value (130km), this value shall not be changed for the rest of the mission because it impacts significantly L2 products quality.

The planned GOMOS operations for the reporting period are identified in table 4.1-2. The operation scenario of GOMOS since 29th August 2005 until end of reporting month consists of:

- Planning 2 orbits per sequence (nominal were 5): this is done because in case of a voice coil failure with subsequent loss of star observation, the maximum loss of consecutive observations cannot exceed two orbits.

- Reduced azimuth field of view (nominal was [-10°, +90°]): as the anomaly occurs during the rallying of the telescope in the preparation for the star observation, it has been decided to reduce the field of view in order to minimize the failure occurrence probability. Different ranges have been used during the reporting period (table 4.1-1) in order to optimize the number of occultations per orbit.

Table 4.1-2: GOMOS planned operations. The planning is built on a 2-orbit sequence basis (2 orbits with the same stars)

UTC Start	Start Orbit	Stop Orbit	Mode (Asynchronous or Synchronous)	Calibration (CAL) Dark Sky Area (DSA) or Nominal (Nom)
01 feb 2007 03.18.32	25738	25777	S	**Nom; Altitude = [130;5]Km**
03 feb 2007 22.22.29	25778	25778	A	**Nom; Altitude = [130;5]Km**
04 feb 2007 01.43.41	25780	25877	S	**Nom; Altitude = [130;5]Km**
11 feb 2007 01.23.34	25880	25977	A	**Nom; Altitude = [130;5]Km**
18 feb 2007 01.03.26	25980	25987	CAL 86	**Nom; Altitude = [130;5]Km**
18 feb 2007 14.28.14	25988	25989	CAL 86	**Nom; Altitude = [130;5]Km**
18 feb 2007 17.49.26	25990	26077	S	**Nom; Altitude = [130;5]Km**
24 feb 2007 21.22.07	26078	26078	A	**Nom; Altitude = [130;5]Km**
25 feb 2007 00.43.19	26080	26177	S	**Nom; Altitude = [130;5]Km**

There was no new Configurable Table Interface (CTI) uploaded to the instrument. The files used since the beginning of the mission are in table 4.1-3.

Table 4.1-3: Historic CTI Tables

CTI filename	Dissemination to FOCC
CTI_SMP_GMVIEC20030716_123904_00000000_00000004_20030715_000000_20781231_235959.N1	16-JUL-2003
CTI_SMP_GMVIEC20021104_075734_00000000_00000003_20021002_000000_20781231_235959.N1	06-NOV-2002
CTI_SMP_GMVIEC20021002_082339_00000000_00000002_20021002_000000_20781231_235959.N1	07-OCT-2002
CTI_SMP_GMVIEC20020207_154455_00000000_00000000_20020301_032709_20781231_235959.N1	21-FEB-2002

4.2 Limb, Illumination conditions and instrument gain setting

The **limb** and the **illumination condition** are two parameters that can confuse the user community. In table 4.2-1 there are specified the product parameter (level 1b and level 2 of processor GOMOS/4.02 operational until 8th August 2006) where the flag is located, the meaning and the source. The difference between the limb (SPH/bright_limb) and the illumination condition (SUMMARY_QUALITY/limb_flag) is that the first

one is coming from the mission scenario and the second is coming from the processing (defined from the computation of the sun zenith and azimuth angles at both instrument and tangent point locations). The SPH/bright_limb is for some occultations set to "dark" in the mission scenario while they are in fact in bright limb illumination conditions. To select the highest quality data for scientific applications, data with SUMMARY_QUALITY/limb_flag equal to '0' should be used (see also the disclaimer: http://envisat.esa.int/dataproducts/availability/disclaimers). The instrument gain settings are also specified in table 4.2-1 (they depend on the mission scenario flags) just for completeness of information.

Table 4.2-1: Relationship between limb, illumination condition flags and instrument gain settings (IPF version GOMOS/4.02 operational until 8 August 2006)

Products parameter	SPH/bright_limb	0 = Dark	1 = Bright	Coming from mission scenario
	SUMMARY_QUALITY/limb_flag	0 = Full Dark 1 = Bright 2 = Twilight	1 = Bright 2 = Twilight	In the geolocation process the sun zenith angle is computed and the occultation then is flagged accordingly
Instrument Gain	SPA Gain	3 (2)	0	Gain setting for spectrometer A. In parenthesis, values valid only for Sirius occultations (starID=1)
	SPB Gain	0	0	Gain setting for spectrometer B

The same is valid for the prototype version GOPR_6.0a_6.0a and following ones (including the one that is used for the on-going second reprocessing of 2002-2005 years), where the **limb** is in fields SPH/bright_limb and SUMMARY_QUALITY/dark_bright_limb and the **illumination condition** is in field SUMMARY_QUALITY/obs_ill_cond. For these prototypes **and the processor GOMOS/5.00 in operations since 8th August 2006**, the illumination condition can have five values (see table 4.2-2).

Table 4.2-2: Relationship between limb, illumination condition flags and instrument gain settings (prototype version GOPR 6.0a_6.0a and following ones)

Products parameter	SPH/bright_limb SUMMARY_QUALITY/dark_bright_limb	0 = Dark	1 = Bright	Coming from mission scenario
	SUMMARY_QUALITY/obs_ill_cond	0 = Full Dark 1 = Bright 2 = Twilight 3 = Straylight 4 = Twi.+Stray		In the geolocation process the sun zenith angle is computed and the occultation is then flagged accordingly
Instrument Gain	SPA Gain	3 (2)	0	Gain setting for spectrometer A. In parenthesis, values valid only for Sirius occultations (starID=1)
	SPB Gain	0	0	Gain setting for spectrometer B

4.3 Thermal Performance

Since the beginning of the mission, the hot pixel and RTS phenomena have been producing a continuous increase of the dark charge signal within the CCD detectors (see section 4.5.1). In order to minimize this effect, three successive CCD cool downs were performed in orbits 800 (25th April 2002), 1050 (13th May 2002) and 2780 (11th September 2002) with a total decrease in temperature of 14 degrees.

Fig. 4.3-1 and 4.3-2 display, respectively, the overall temperature variation and the temperature variation around the Ascending Node Crossing (ANX) time with a resolution of 0.4 degrees (coding accuracy for level 0 data). The CCD temperatures show the expected global increase due to the radiator ageing.

Another expected variation of the temperatures, the seasonal one, with amplitude of around 0.8 degrees, can be also observed. The peaks that occur mainly in spectrometer B1 and B2 are also to be noted. They happen a little before the ANX for some consecutive orbits and every 8-10 days. Their origin is not known, as we did not find any correlation between these peaks and other activities carried out by other ENVISAT instruments. The CCD temperature at almost the same latitude location (fig. 4.3-2) is monitored in order to detect any inter-orbital temperature variation. The abnormal decreases observed sometimes in all detectors are after GOMOS switch off periods, when the instrument did not have enough time to reach the nominal temperature before starting the measurements.

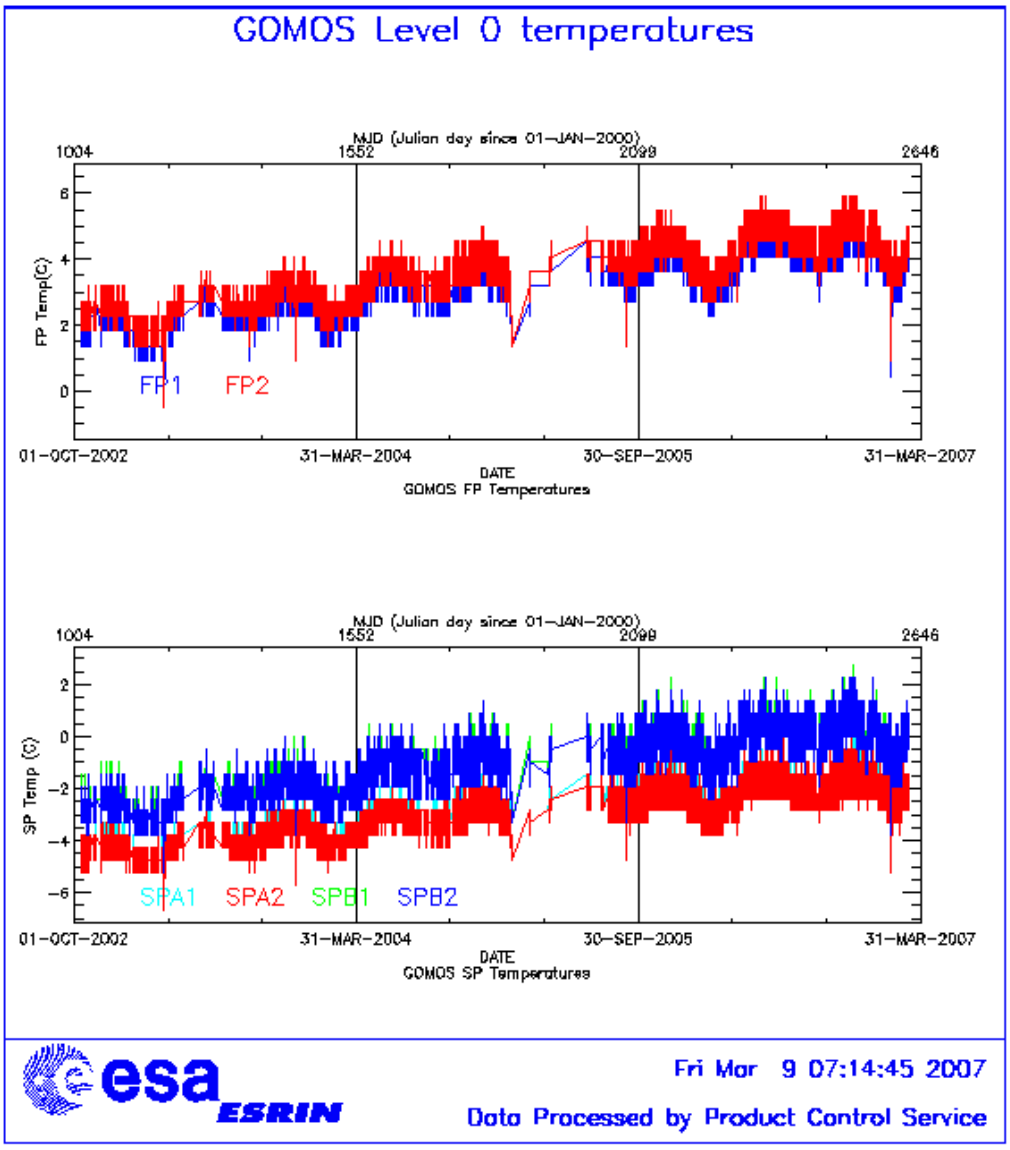

Figure 4.3-1: Level 0 temperature evolution of all GOMOS CCD detectors since October 2002 until the end of the reporting period

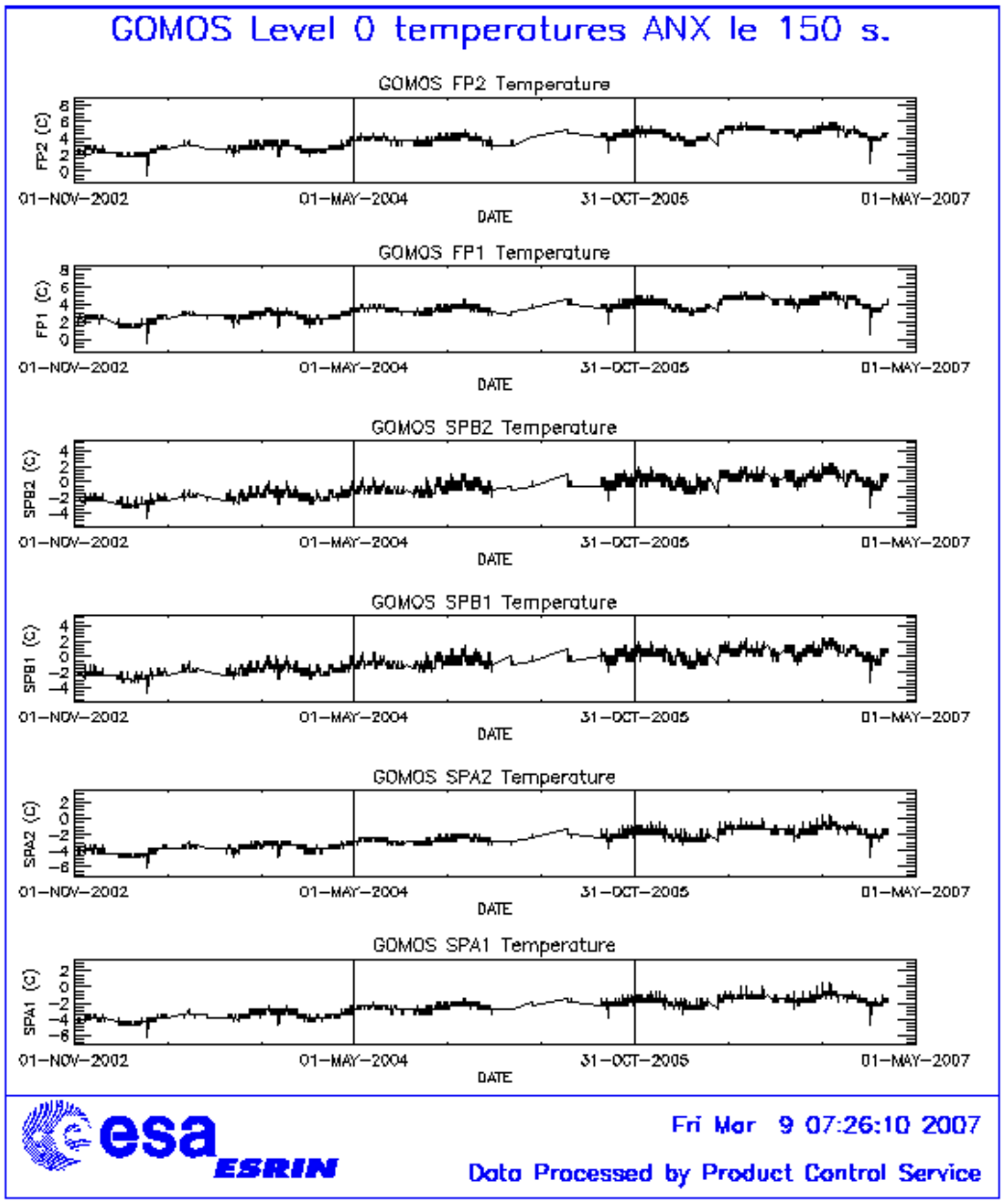

Figure 4.3-2: Level 0 temperature evolution of all GOMOS CCD detectors around ANX since November 2002 until the end of the reporting period

During the reporting period, the orbital temperature variation of the detector SPB2 for ascending and descending passes (fig. 4.3-3 and 4.3-4) is nominal, around 2.5-3 degrees. The stability of the temperature during the orbit is important because it affects the position of the interference patterns. The phenomenon of the interference is present mainly in SPB and this Pixel Response Non-Uniformity (PRNU) is corrected during the processing.

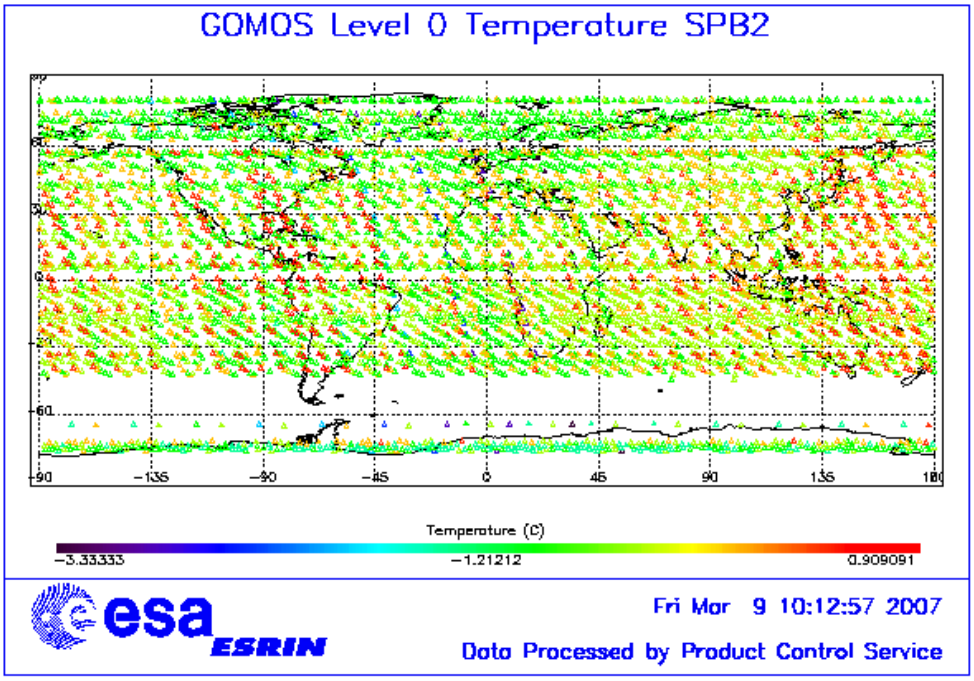

Figure 4.3-3: Ascending orbital variation of SPB2 temperature during reporting period

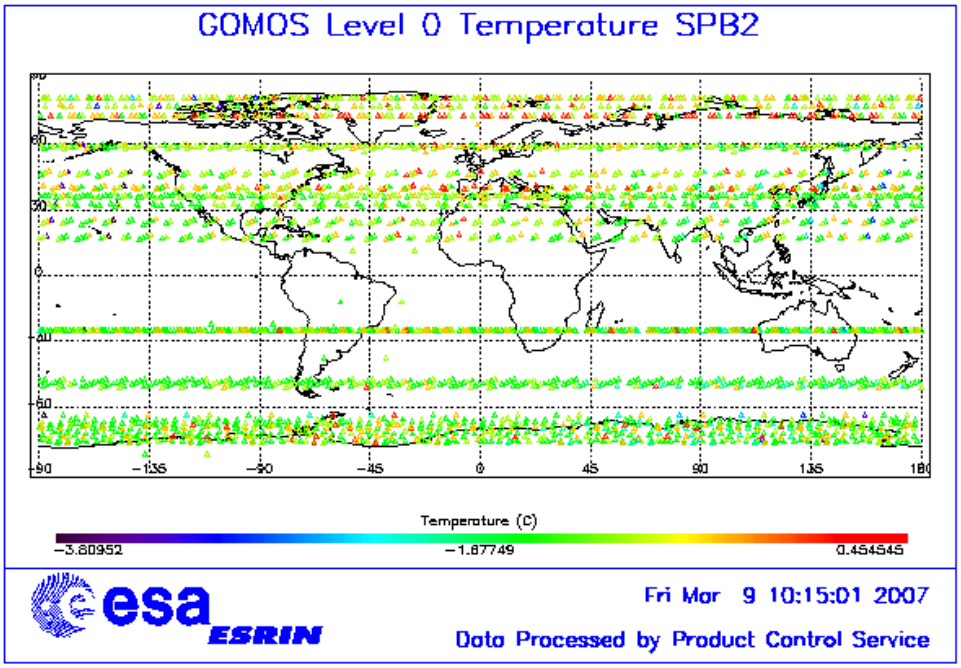

Figure 4.3-4: Descending orbital variation of SPB2 temperature during reporting period

4.4 Optomechanical Performance

New band setting calibration has been performed during the reporting period.

- Version GOMOS/4.00 and previous ones: in the GOMOS processor versions GOMOS/4.00 and previous, the spectra are expected to be aligned along CCD lines, and therefore use only a single average line index per CCD. In table 4.4-1, the mean values of the location of the star signal for all the calibration analysis done is reported. The 'left' and 'right' values are calculated (the whole interval is not used) because the spectra present a slight slope, more pronounced in spectrometer B (see fig. 4.4-1). In table 4.4-2, mean values of the location of the star signal are calculated for some specific wavelength intervals. These intervals have been changed between the calibration performed in September 2002 and the ones performed afterwards (until November 2003). Table 4.4-3 reports the average location of the star spot on the photometer 1 and 2 CCD.

- Version GOMOS/4.02: in this processor version (GOMOS/4.02) operational since 23rd March 2004 to 8th August 2006, a Look Up Table (LUT) gives the line index of the spectra location as a function of the wavelength. However this characterization curve is not exactly the location of the star spectrum on the CCD but rather a combination of this position and some artefact created by the shape of the instrument optical point spread function (PSF). The exact shape is actually a straight line (especially for SPB) that has been characterised in 2005.

- Current version GOMOS/5.00 (since 8th August 2006): the exact shape of the CCD spectra location curve (which is a straight line) that has been characterised in 2005 was implemented in the current set of GOMOS ADFs. The position of the spectra convoluted with the PSF is calculated during the processing.

Table 4.4-1: Mean value of the location of the star signal during the occultation at the edges of every band (mean over 50 values, filtering the outliers)

	UV (SPA1) left/right	VIS (SPA2) left/right (Inverted spectra)	IR1 (SPB1) left/right	IR2 (SPB2) left/right
11/09/2002	80.7/80.7	79.8/79.5	82.8/81.9	83.1/82.1
01/01/2003	80.7/80.6	79.8/79.5	82.8/82.0	83.2/82.2
17/07/2003 & 02/08/2003	80.7/80.7	79.8/79.5	82.8/81.9	83.1/82.1
08/11/2003	80.7/80.6	79.8/79.5	82.8/81.9	83.1/82.1

Table 4.4-2: Mean value of the location of the star signal during the occultation (as table 4.4-1) but now within some wavelength intervals

	UV (SPA1)	VIS (SPA2)	IR1 (SPB1)	IR2 (SPB2)
11/09/2002 wl range (nm)	80.8 [300-330]	79.8 [500-530]	82.6 [760-765]	82.9 [937-942]
01/01/2003 wl range (nm)	80.6 [350-360]	78.6 [650-670]	81.6 [760-765]	80.3 [935-945]
02/08/2003	80.6	79.7	82.5	82.8
08/11/2003	80.6	79.9	82.4	82.8

Table 4.4-3: Average column and row pixel location of the star spot on the photometer CCD during the occultation

	FP1 (column/row)	FP2 (column/row)
11/09/2002	11/4	5/5
01/01/2003	10/4	6/4.9
02/08/2003	10/4	6/5
08/11/2003	10/4	6/5

Table 4.4-4: Location of the star signal on the CCD's (corresponding to fig. 4.4-1)

Pixel Column	LUT (Pixel line)	Calibration on 10-APR-2004	Calibration on 04-DEC-2004	Calibration on 27-NOV-2005	Calibration on 19-FEB-2006	Calibration on 14-MAY-2006 and 11-JUN-2006
0	**80.59**	80.80	80.67	80.93	80.67	80.85
20	**80.46**	80.60	80.44	80.32	80.43	80.49
449	**80.42**	80.50	80.42	80.40	80.53	80.56
450	**79.25**	79.39	79.30	79.16	79.30	79.35
900	**79.50**	79.63	79.57	79.36	79.45	79.61
1415	**79.70**	79.76	79.76	80.00	79.81	79.93
1416	**82.64**	82.80	82.88	82.95	82.76	82.81
1500	**82.31**	82.60	82.66	82.63	82.58	82.55
1600	**82.12**	82.22	82.30	82.35	82.41	82.20
1700	**81.97**	82.04	82.08	82.09	82.05	82.06
1750	**81.89**	81.98	82.03	82.00	81.92	81.97
1800	**81.78**	81.91	81.96	81.93	81.83	81.98
1835	**81.68**	81.88	81.94	81.96	81.79	81.91
1836	**82.98**	83.10	83.10	83.27	83.17	83.08
2000	**82.78**	82.90	82.94	83.04	82.83	82.93
2100	**82.33**	82.70	82.73	82.82	82.83	82.67
2150	**82.17**	82.40	82.54	82.79	82.70	82.49
2350	**81.83**	82.00	82.00	82.68	81.96	82.11

4.5 Electronic Performance

4.5.1 DARK CHARGE EVOLUTION AND TREND

The trend of Dark Charge (DC) is of crucial importance for the final quality of the products, and is therefore subject to intense monitoring. As part of the DC there is:

- "Hot pixels", a pixel is "hot" when its dark charge exceeds its value measured on ground, at the same temperature, by a significant amount.
- RTS phenomenon (Random Telegraphic Signal), it is an abrupt change (positive or negative) of the CCD pixel signal, random in time, affecting only the DC part of the signal and not the photon generated signal.

The temperature dependence of the DC would make this parameter a good indicator of the DC behaviour, but the hot pixels and the RTS are producing a continuous increase of the DC (see trend in fig. 4.5-1 and 4.5-2). To take into account these phenomena, since version GOMOS/4.00 (the current one is GOMOS/5.00) a DC map per orbit is extracted from a Dark Sky Area (DSA) observation performed around

ANX (full dark conditions). For every level 1b product (occultation), the actual thermistor temperature of the CCD is used to convert the DC map measured around ANX into an estimate of the DC at the time (and different temperature) of the actual occultation. When the DSA observation is not available, the DC map inside the calibration product that was measured at a given thermistor reference temperature is used; again, the actual thermistor temperature of the CCD is used to compute the actual map. Table 4.5-1 reports the list of products that used the DC maps inside the calibration file due to the non-availability of DSA observation. A "CAL DC map with no T dep." means that, as the temperature information was not available for that occultation, the DC map used is exactly the one inside the Calibration product.

The "quality ranking" of the products depending on DC correction performed is as follows:

- Best quality: products with DC correction using DSA observation inside the orbit
- Less quality than previous ones: products with DC correction using the map inside the calibration product, thermal corrected ('DC map used' in table 4.5-1)
- Less quality than previous ones: products with DC correction using the map inside the calibration product, no thermal corrected ('DC map with no T dep.' in table 4.5-1)

Table 4.5-1: Table of level 1b products that used the Calibration DC maps instead of the DSA observation

Product name	DC information
GOM_TRA_1PNPDE20070202_194648_000000422055_00157_25762_2913.N1	DC map used
GOM_TRA_1PNPDE20070202_194832_000000422055_00157_25762_2914.N1	DC map used
GOM_TRA_1PNPDE20070202_195103_000000412055_00157_25762_2915.N1	DC map used
GOM_TRA_1PNPDE20070202_195308_000000392055_00157_25762_2916.N1	DC map used
GOM_TRA_1PNPDE20070202_195429_000000412055_00157_25762_2917.N1	DC map used
GOM_TRA_1PNPDE20070202_195655_000000422055_00157_25762_2918.N1	DC map used
GOM_TRA_1PNPDE20070202_195818_000000382055_00157_25762_2919.N1	DC map used
GOM_TRA_1PNPDE20070202_200027_000000432055_00157_25762_2920.N1	DC map used
GOM_TRA_1PNPDE20070202_200611_000000502055_00157_25762_2921.N1	DC map used
GOM_TRA_1PNPDE20070202_200941_000000372055_00157_25762_2922.N1	DC map used
GOM_TRA_1PNPDE20070202_201131_000000382055_00157_25762_2923.N1	DC map used
GOM_TRA_1PNPDE20070202_201351_000000382055_00157_25762_2924.N1	DC map used
GOM_TRA_1PNPDE20070202_201551_000000352055_00157_25762_2925.N1	DC map used
GOM_TRA_1PNPDE20070202_201755_000000352055_00157_25762_2926.N1	DC map used
GOM_TRA_1PNPDE20070202_203005_000000372055_00157_25762_2927.N1	DC map used
GOM_TRA_1PNPDE20070202_204118_000000392055_00157_25762_2928.N1	DC map used
GOM_TRA_1PNPDE20070202_204445_000000372055_00157_25762_2929.N1	DC map used
GOM_TRA_1PNPDE20070202_205125_000000332055_00157_25762_2930.N1	DC map used
GOM_TRA_1PNPDE20070204_000115_000000382055_00173_25778_4055.N1	DC map used
GOM_TRA_1PNPDE20070204_042746_000000482055_00176_25781_4531.N1	DC map used
GOM_TRA_1PNPDE20070204_043346_000000322055_00176_25781_4532.N1	DC map used
GOM_TRA_1PNPDE20070204_043610_000000372055_00176_25781_4533.N1	DC map used
GOM_TRA_1PNPDE20070204_045524_000000422055_00176_25781_4534.N1	DC map used
GOM_TRA_1PNPDE20070204_045636_000000402055_00176_25781_4535.N1	DC map used
GOM_TRA_1PNPDE20070205_195247_000000372055_00200_25805_6088.N1	DC map with no T dep.
GOM_TRA_1PNPDE20070205_195429_000000422055_00200_25805_6089.N1	DC map used
GOM_TRA_1PNPDE20070205_195658_000000402055_00200_25805_6090.N1	DC map used

GOM_TRA_1PNPDE20070205_195902_000000392055_00200_25805_6091.N1	DC map used
GOM_TRA_1PNPDE20070205_200021_000000422055_00200_25805_6092.N1	DC map used
GOM_TRA_1PNPDE20070205_200247_000000412055_00200_25805_6093.N1	DC map used
GOM_TRA_1PNPDE20070205_200410_000000392055_00200_25805_6094.N1	DC map used
GOM_TRA_1PNPDE20070205_200621_000000502055_00200_25805_6095.N1	DC map used
GOM_TRA_1PNPDE20070205_201158_000000472055_00200_25805_6096.N1	DC map used
GOM_TRA_1PNPDE20070205_201534_000000372055_00200_25805_6097.N1	DC map used
GOM_TRA_1PNPDE20070205_201727_000000382055_00200_25805_6098.N1	DC map used
GOM_TRA_1PNPDE20070205_202148_000000532055_00200_25805_6099.N1	DC map used
GOM_TRA_1PNPDE20070205_202351_000000352055_00200_25805_6100.N1	DC map used
GOM_TRA_1PNPDE20070205_203551_000000362055_00200_25805_6101.N1	DC map used
GOM_TRA_1PNPDE20070205_204215_000000332055_00200_25805_6102.N1	DC map used
GOM_TRA_1PNPDE20070205_204813_000000512055_00200_25805_6103.N1	DC map used
GOM_TRA_1PNPDE20070205_205036_000000332055_00200_25805_6104.N1	DC map used
GOM_TRA_1PNPDE20070205_205718_000000322055_00200_25805_6105.N1	DC map used
GOM_TRA_1PNPDE20070215_193903_000000402055_00343_25948_8752.N1	DC map with no T dep.
GOM_TRA_1PNPDE20070215_194040_000000412055_00343_25948_8753.N1	DC map used
GOM_TRA_1PNPDE20070215_194303_000000412055_00343_25948_8754.N1	DC map used
GOM_TRA_1PNPDE20070215_194508_000000402055_00343_25948_8755.N1	DC map used
GOM_TRA_1PNPDE20070215_194926_000000402055_00343_25948_8756.N1	DC map used
GOM_TRA_1PNPDE20070215_195753_000000472055_00343_25948_8757.N1	DC map used
GOM_TRA_1PNPDE20070218_194458_000000362055_00386_25991_2783.N1	DC map used
GOM_TRA_1PNPDE20070218_194919_000000422055_00386_25991_2784.N1	DC map used
GOM_TRA_1PNPDE20070218_200959_000000382055_00386_25991_2785.N1	DC map used
GOM_TRA_1PNPDE20070218_201108_000000372055_00386_25991_2786.N1	DC map used
GOM_TRA_1PNPDE20070218_202718_000000362055_00386_25991_2787.N1	DC map used
GOM_TRA_1PNPDE20070218_204004_000000342055_00386_25991_2788.N1	DC map used
GOM_TRA_1PNPDE20070218_204219_000000402055_00386_25991_2789.N1	DC map used
GOM_TRA_1PNPDE20070218_204921_000000342055_00386_25991_2790.N1	DC map used
GOM_TRA_1PNPDE20070223_015255_000000462055_00447_26052_8770.N1	DC map with no T dep.

The average DC inserted by the processor into the level 1b data products for the spectrometers SPA1 and SPB2 (per band: upper, central and lower) is plotted in fig. 4.5-1 and 4.5-2. From the figures, it can be noted that the DC increase is similar throughout the mission.

The same DC values are plotted in fig. 4.5-3 but for some occultations belonging only to the reporting month.

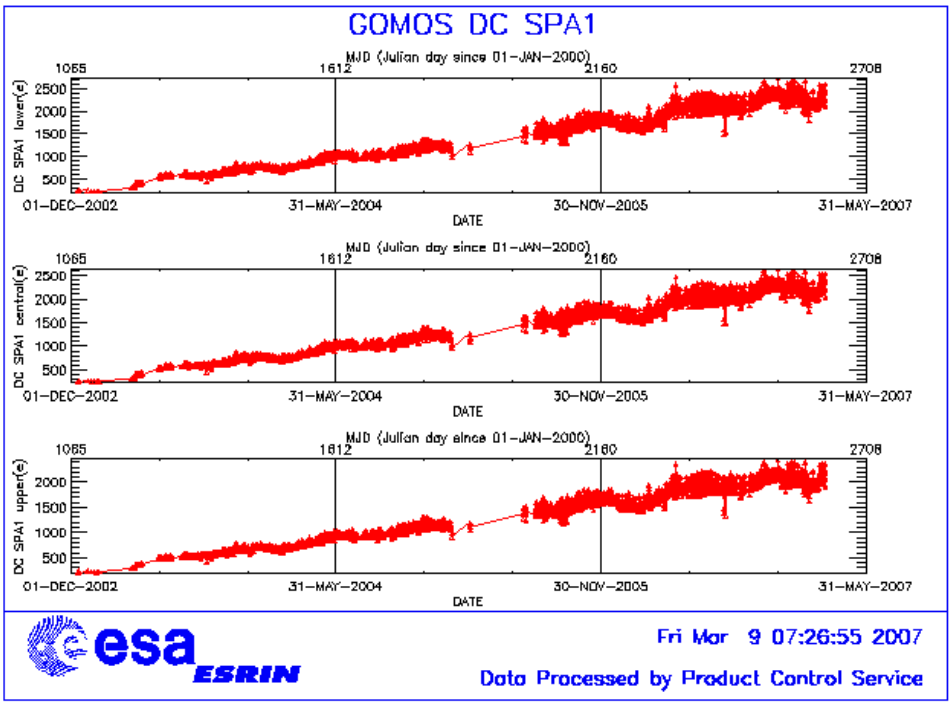

Figure 4.5-1: Mean DC evolution on SPA1 since 15th December 2002 until the end of the reporting period

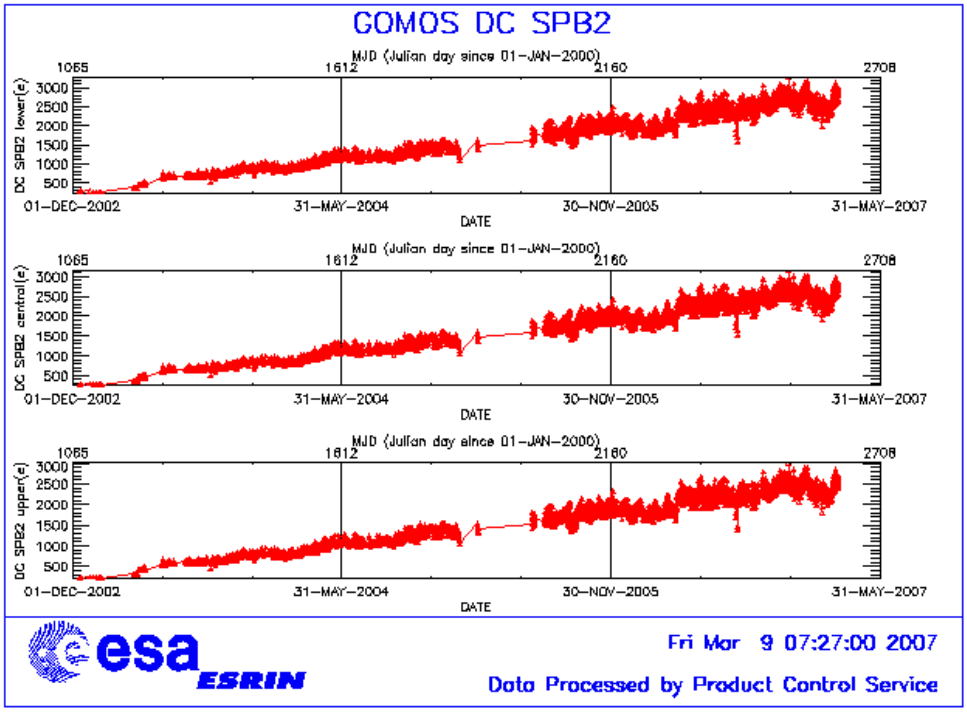

Figure 4.5-2: Mean DC evolution on SPB2 from 15th December 2002 until the end of the reporting period

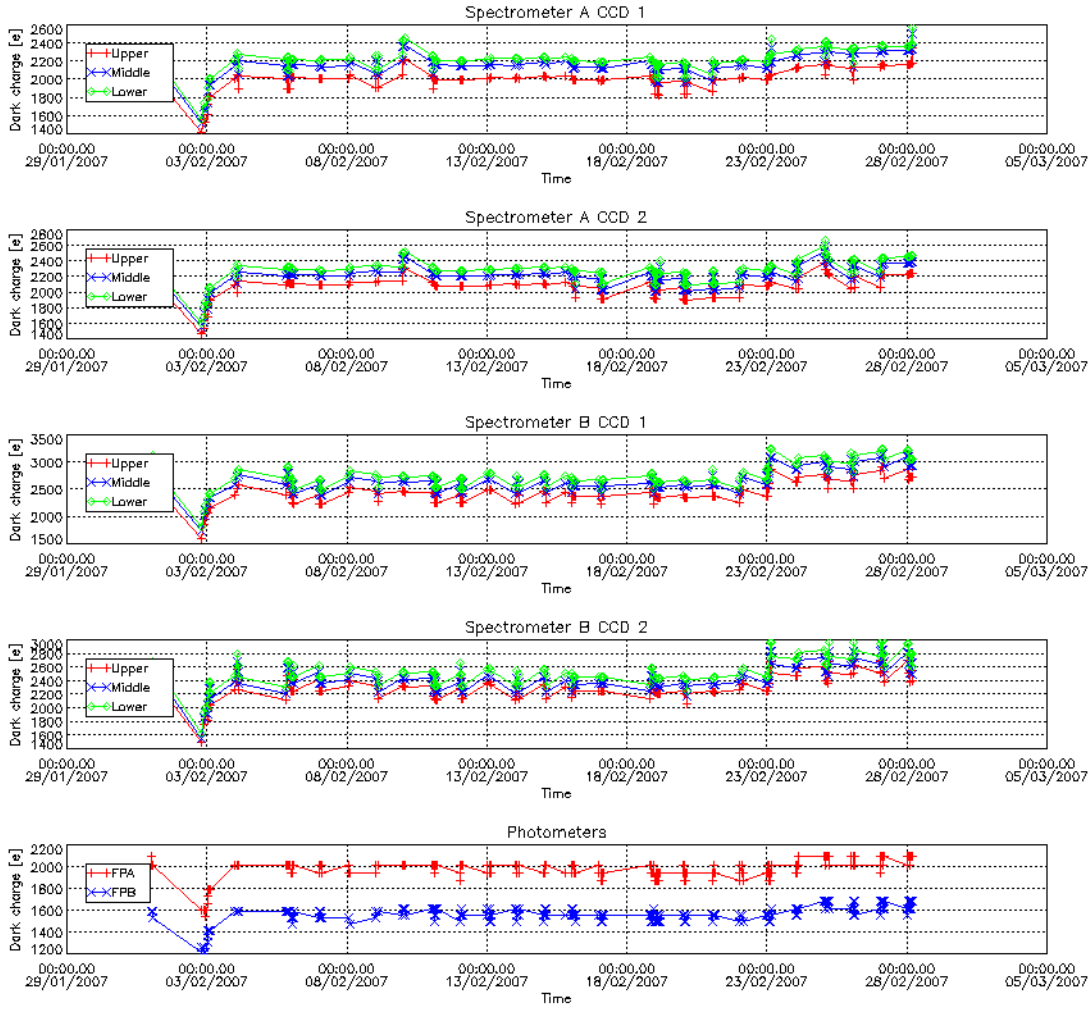

Figure 4.5-3: Mean Dark Charge of spectrometers during the reporting period

4.5.2 SIGNAL MODULATION

A parasitic signal was found to be systematically present, added to the useful signal, for the spectrometers A and B. The modulation is corrected in the data processing for spectrometers A1 and A2 (for spectrometer B it has much smaller amplitude and so is not corrected) and the modulation signal standard deviation is routinely monitored in order to detect any trend (fig. 4.5-4).

The modulation standard deviation, for every spectrometer, is characterised as follows:

$$\sigma_{mod} = (\text{'static noises'} - \text{'total static variance'})^{1/2} / \text{gain} \qquad \text{(in ADU)}$$

- The 'static noises' are calculated from the DSA observation performed once per orbit
- The 'total static variance' is obtained from ADF data (electronic chain noise, quantization noise).

The standard deviation of the modulation signal (fig. 4.5-4) shows high values during summer time for the ESRIN data, it now being confirmed that the South Atlantic Anomaly is the cause of these unexpected peaks. The quality of ESRIN data, in particular over the SAA zone, is impacted but the measure of this impact is under investigation. However, in the second half of the months of October (2004, 2005 and 2006) the peaks are smaller because the DSA zone where the data are taken for this analysis is moving towards the Northern Hemisphere. At the end of October the DSA zone is definitely chosen by the planning system in the Northern Hemisphere (to fill the criteria 'DSA in full dark limb conditions') and the high peaks disappear.

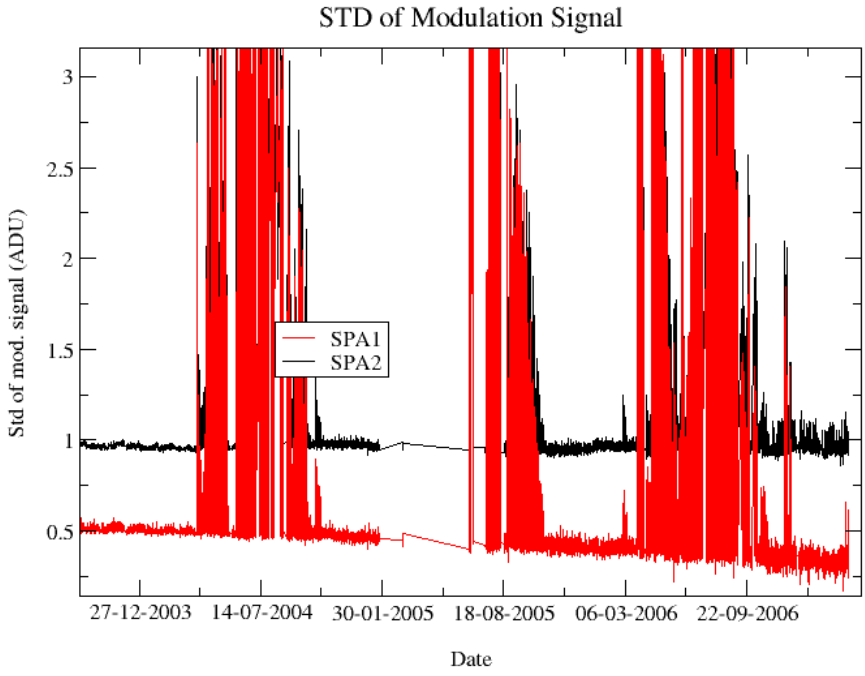

Figure 4.5-4: Standard deviation of the modulation signal

The QWG team has checked if the trend observed mainly for SPA1 in fig. 4.5-4 has an impact on the GOMOS products quality. The conclusion is that the differences between the current amplitudes and the values used in the data processing are too small to have a significant impact on the retrieval.

4.5.3 ELECTRONIC CHAIN GAIN AND OFFSET

No new electronic chain gain and offset calibration has been done during the reporting period so the results have been presented in previous MR.

The routine monitoring of the ADC offset is a good indicator of the ageing of the instrument electronics. During November 2005 an exercise has been done to analyze the variation of the ADC offset using the calibration observation in linearity mode performed on 28th November 2005.

The fig. 4.5-7 presents the evolution of the calibrated ADC offset for each spectrometer electronic chain. The unexpected increase of this offset seems to be due to an external contribution. In the ADC offset calibration procedure, linearity observations are used with two integration times of 0.25 and 0.50 seconds to extrapolate to an integration time of 0 seconds that gives the complete chain offset and not only the ADC offset. The complete offset contains any possible offsets, and especially the static dark charge (i.e. the dark charge that does not depend on the spectrometer integration time). If the memory area of the CCD is affected by the generation of hot pixels (this is confirmed by the presence of vertical lines visible in the measurement maps in spatial spread monitoring mode), it can be concluded that the increase observed in fig. 4.5-5 is due to these new hot pixels.

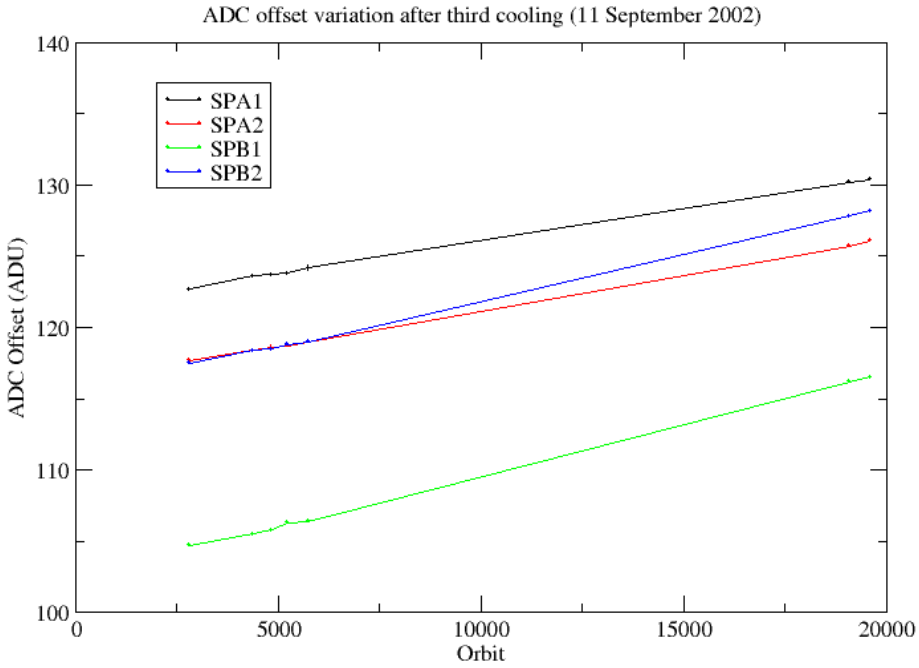

Figure 4.5-5: Evolution of the ADC offset for each spectrometer electronic chain

A current QWG task consists in completing the analysis to confirm that the offset increase is due to the dark charge increase in the memory area. This can be proven by the study of the noise due to the increased dark charge. The increase of ADC offset will be assumed to be equal to the increase of 'static dark charge' and the corresponding noise will be computed and compared to the increase of the residual of the signal variance.

If we keep the ADC offset constant, as it is also used to compute the dark charge at band level (which is used to correct the samples in the level 1b processing), the increase of the static dark charge - not taken into account in the ADC offset - is compensated by an artificial increase of the calibrated dark charge. So, the star and limb spectra are correctly corrected for dark charge. A small bias can be added to the instrument noise due to the incorrect dark charge level. Anyway, this quantity is not large enough to require a modification of the ADC offset value.

4.6 Acquisition, Detection and Pointing Performance

4.6.1 SATU NOISE EQUIVALENT ANGLE

The Star Acquisition and Tracking Unit (SATU) noise equivalent angle (SATU NEA) consists of the statistical angular variation of the SATU data above the atmosphere. The mean of the standard deviation (STD over the 50 values per measurement) above 105 km are computed for every occultation, giving two values per occultation: one in the 'X' direction, one in the 'Y' direction. A mean value per day in every direction and limb is calculated and monitored in order to assess instrument performance in terms of star pointing (fig. 4.6-1, upper). Also monthly averages are calculated and plotted (fig. 4.6-2). The thresholds are 2 and 3 micro radians in 'X' and 'Y' directions respectively. Before May 2003, data above 90 km have been considered (instead of 105 km) but from May 2003 on, data taken in the mesospheric oxygen layer (located around 100 km altitude) have been avoided because they could cause fluctuations on the SATU data. Also the products with errors (error flag set) are discarded from May 2003 onwards.

As can be seen in fig. 4-6.1, the SATU NEA had a sudden increase on 8th September 2005 mainly in 'Y' axis. These values remained high, fluctuating between 1 and 1.8 microrad until December 2005 when they came back to the values they used to be before the increase of September. The reason why there was higher noise in the data causing the jump in daily SATU average is not known.

Now a different problem has been present since mid April 2006. A gradual increase of the daily SATU Y mean is observed. This increase is due to fluctuations of the SATU 'Y' data observed at the beginning of the occultations (starting at 130 km that corresponds to an elevation angle of around 65^{o}). The decrease of the start elevation angle of the occultation has no impact on the amplitude of the SATU-Y fluctuations. Preliminary investigations carried out by the ESL, ESA and industry point to a problem on the SFM (mechanical or electrical) and not to a problem on the SATU itself. Since mid June the increase was stable for a while at around 5.5 micro radians. The evolution of the anomaly can be summarized as follows:

1) Mid April – mid June: gradual increase until 5.5 microrad (unknown reason of the fluctuations)
2) Mid June – mid July: stability until mid July when it starts to decrease (unknown reason of less fluctuations)
3) Mid July – end August: further decrease due to a change in the start altitude of the occultations, from nominal 130 km to 112.5 km
4) End August – end September: increase and then stability to values found at the end of period 2) due to change in start tangent altitude of the occultations, from 112.5 Km to nominal 130 km. An increase has been observed after the ENVISAT anomaly on 13th September 2006.
5) End November 2006 increase after the ENVISAT switch off of 28 November
6) In the last months the value is stable at around 2.2 micro radians.

The results for some occultations belonging to previous months (monthly averages) are presented in fig. 4.6-2, where the change in trend in September 2005 and May 2006, mainly for the 'Y' axis is visible.

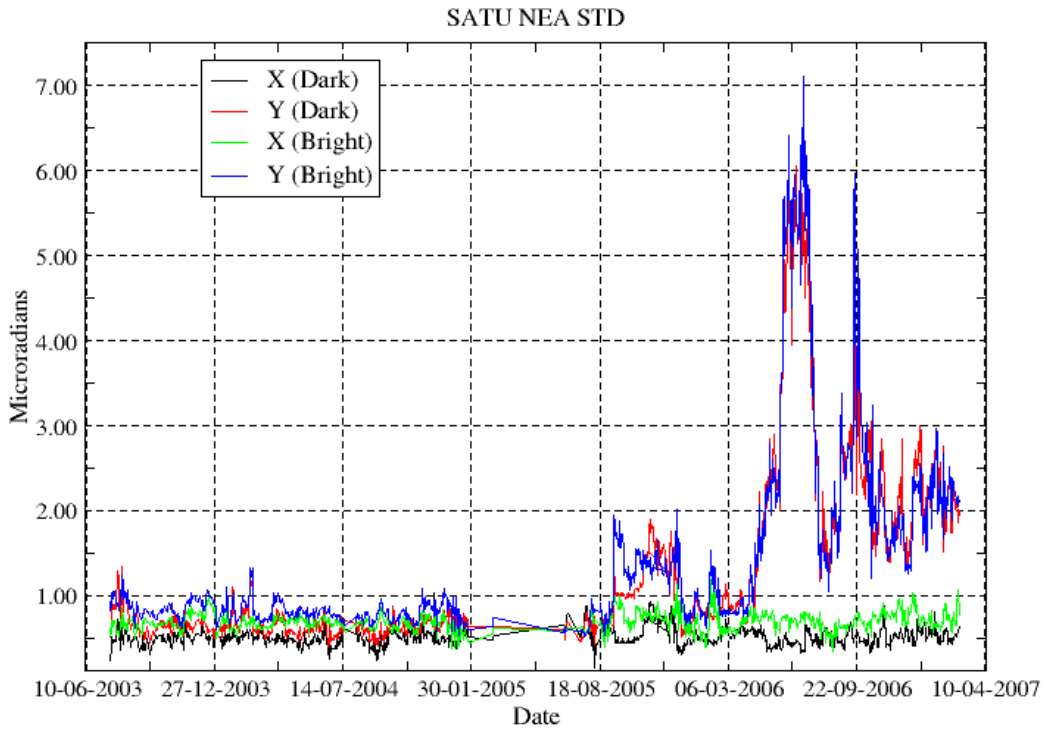

Figure 4.6-1: Average value per day of SATU NEA STD above 105 km

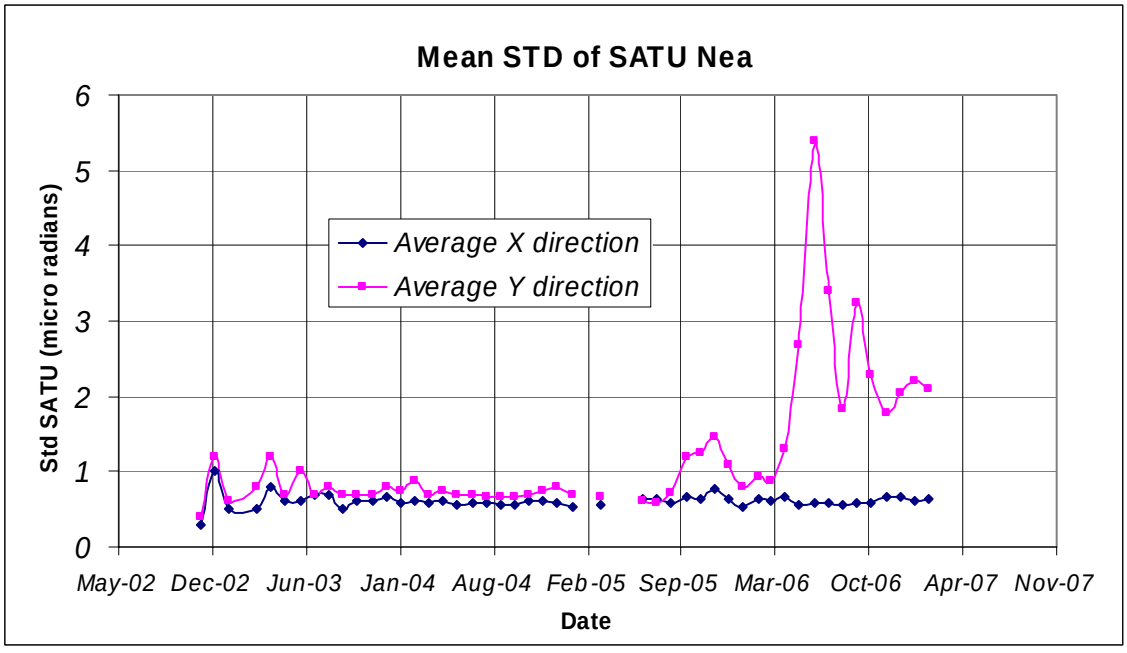

Figure 4.6-2: Average value per month of SATU NEA STD above 105 km

4.6.2 TRACKING LOSS INFORMATION

This verification consists of the monitoring of the tangent altitude at which the star is lost. It is an indicator of the pointing performance although it is to be considered that star tracking is also lost due to the presence of clouds and hence not only due to deficiencies in the pointing performance. Therefore, only the detection of any systematic long-term trend is the main purpose of this monitoring. The recent results are presented in fig. 4.6-3 and 4.6-4:

- The dependence of the altitude at which tracking is lost on the magnitude of the star is very small because the tracking is mainly lost due to the refraction and the scintillation that depend on the atmospheric conditions.
- The azimuth of some stars could be very near to the reduced instrument azimuth edges and therefore there could be occultations planned to have a duration very small (2, 6, 10…seconds).To avoid planning this kind of useless occultation, it has been decided to set the minimum occultation duration value to 25 seconds. Fig. 4.6-4 (bright limb) shows stars lost at altitudes higher than 30 km which corresponds with durations around 25-35 seconds.
- In bright limb it is not expected that the stars are lost at very low altitudes due to the amount of light arriving to the pointing system mainly when the refraction effects start to be important. We see from fig. 4.6-4 that there are some stars lost at altitudes around 4 km. This occurs when the pointing system is not able to point to the star anymore but, instead of finishing the occultation, it continues to track light until the planned duration is reached.
- Daily statistics are given in fig. 4.6-5 (calculated using 50 products per day). The high peaks in standard deviation before 25th January 2005 are due to the long lasting occultations or partial occultations (the entire occultation is included within the following orbit data). The ones during June/July/August 2005 are due to the tests performed for the anomaly investigation. After 29th August the peaks are due to the “short occultations”.
- Monthly statistics are given in fig. 4.6-6 (calculated using 50 products per day) where the change in trends, mainly for dark limb, is visible for the period of GOMOS testing.

Tangent altitude at which the star is lost

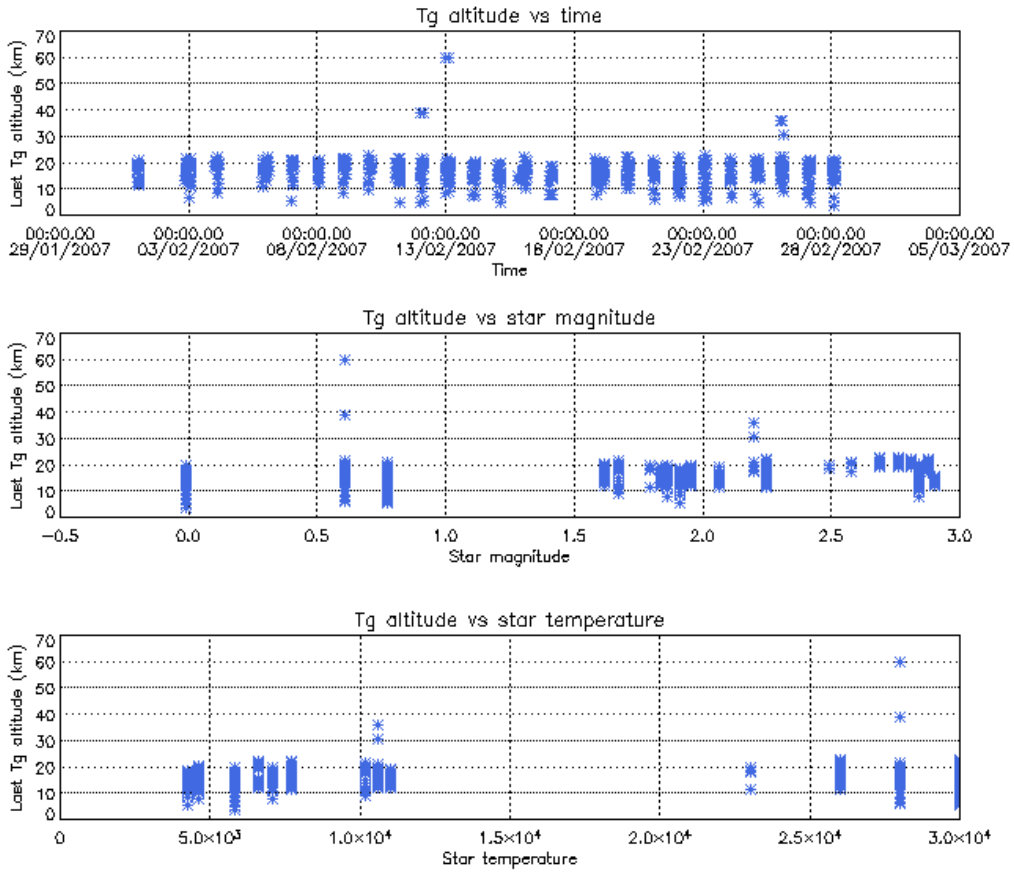

Figure 4.6-3: Last tangent altitude of the occultation (dark limb), point at which the star is lost

Tangent altitude at which the star is lost

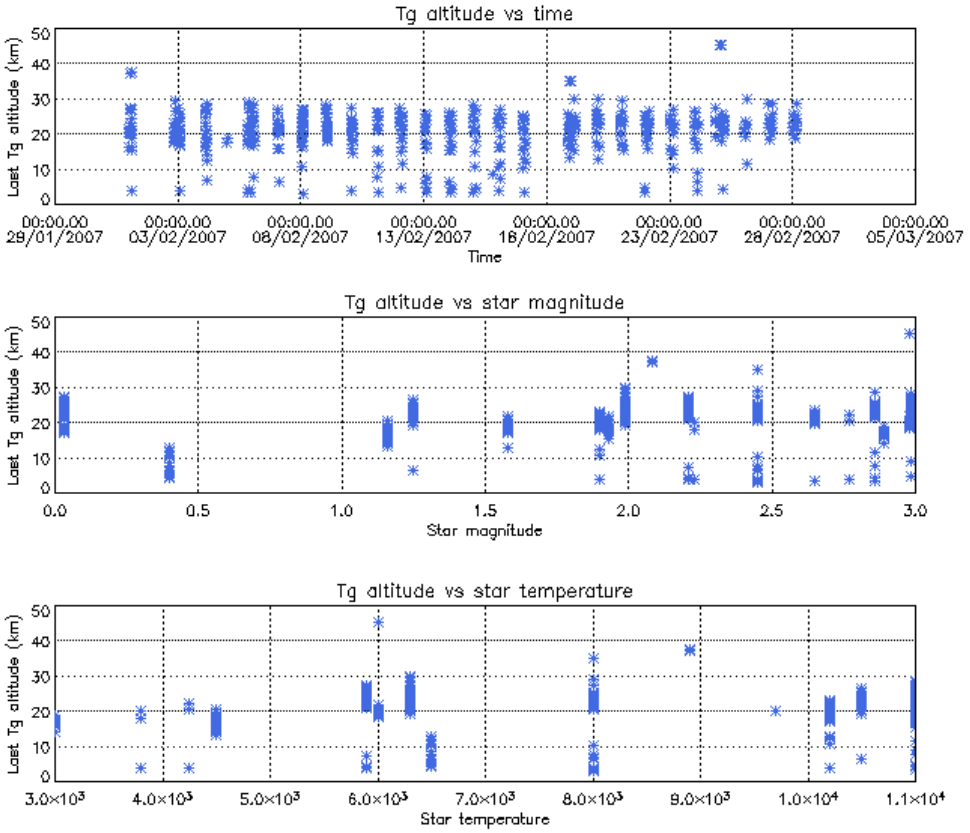

Figure 4.6-4: Last tangent altitude of the occultation (bright limb), point at which the star is lost

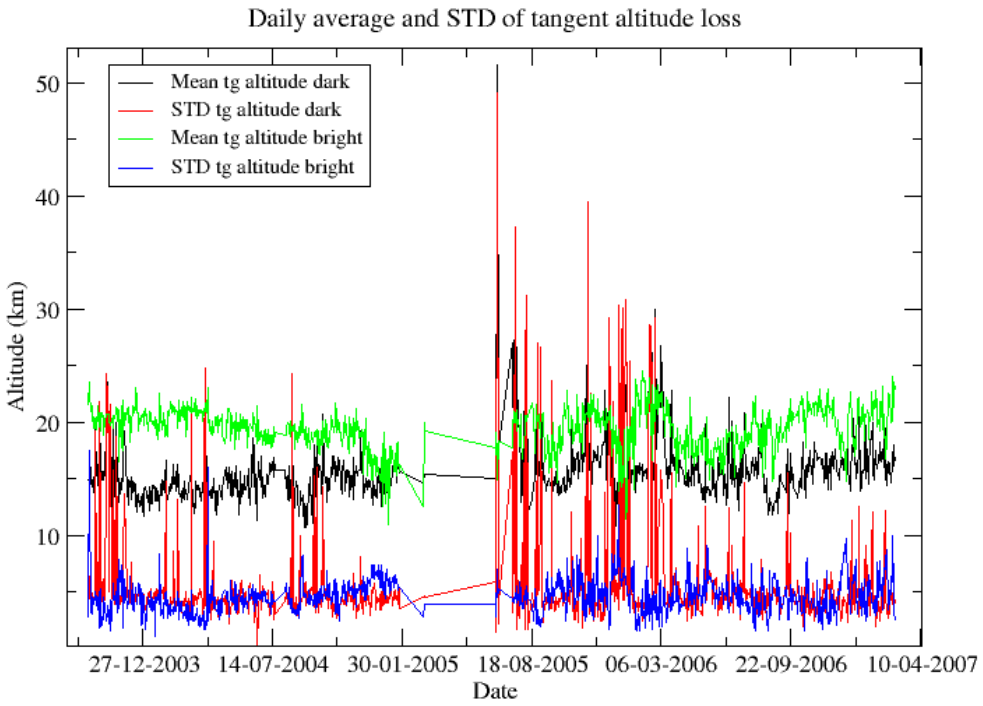

Figure 4.6-5: Daily average and STD of tangent altitude loss for the reporting period

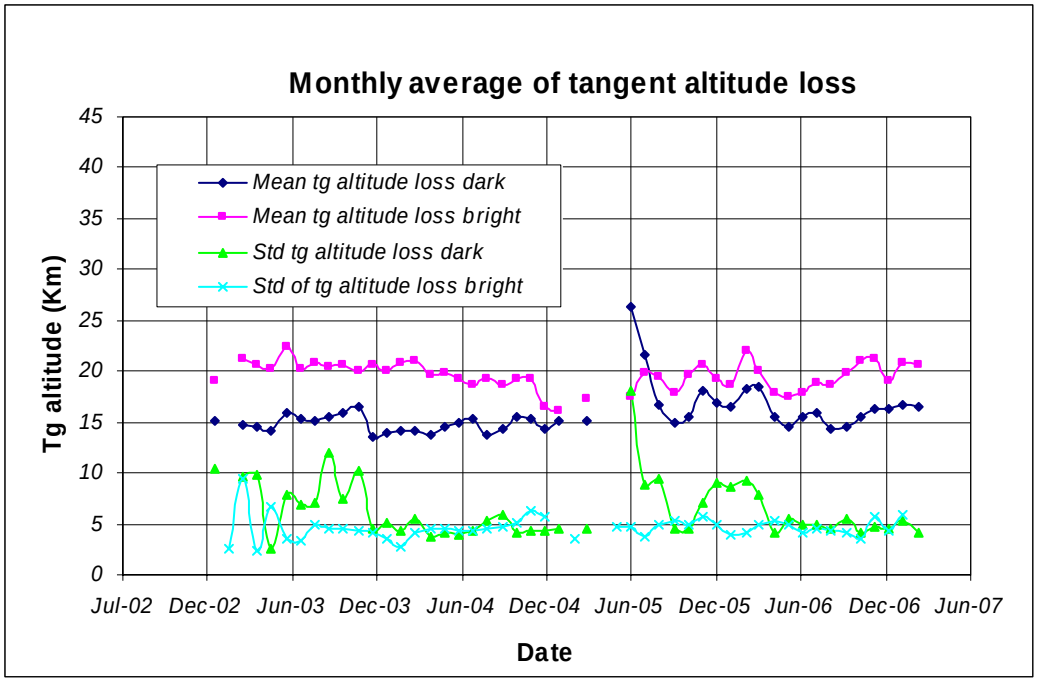

Figure 4.6-6: Monthly mean tangent altitude (and STD) at which the star is lost since January 2003

4.6.3 MOST ILLUMINATED PIXEL (MIP)

The MIP (Most Illuminated Pixel) is the star position on the SATU CCD in detection mode and it is recorded in the housekeeping data. The nominal centre of the SATU is pixel number **145** in elevation and number **205** in azimuth. The detection of the stars should not be far from this centre. As it can be seen in fig. 4.6-7 the **azimuth MIP** was within the threshold (table 4.6-1) since September 2002 until the occurrence of the anomaly on January 2005, even if a small variation is present. The reason for the change in trend observed after the anomaly is, at the moment, not understood. The **elevation MIP** had a significant variation (see the *note* below) until 12th December 2003 when a new PSO algorithm was activated in order to reduce the deviations of the ENVISAT platform attitude with respect to the nominal one. Similarly to the azimuth, after the anomaly of January 2005 the Elevation MIP has a drift that has no explanation. Investigations are ongoing to try to understand this behavior of the MIP as, although it does not impact the data quality or the star location on the CCD array during the measurements, it may invalidate attitude monitoring by GOMOS and could represent a hidden anomaly.

Note: A MIP variation onto the SATU CCD of 50 pixels corresponds to a de-pointing of 0.1 degrees

Table 4.6-1: MIP Thresholds

MIP X	**Mean delta Az**	[198 - 210]
	Std delta Az	7
MIP Y	**Mean delta El**	[140 – 150]
	Std delta El	4

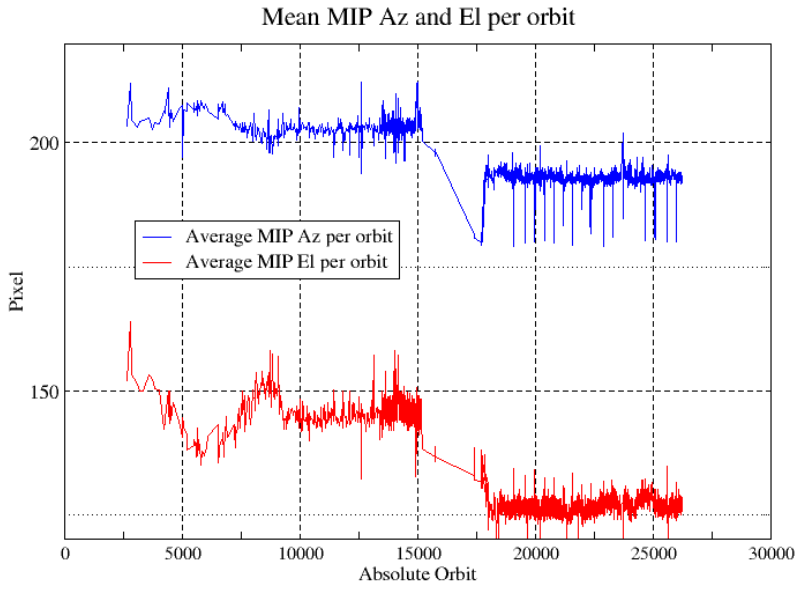

Figure 4.6-7: Mean values of MIP for some orbits since 1st September 2002 (see table 4.6-1)

Fig. 4.6-8 shows the standard deviation of azimuth and elevation MIP that should be within the thresholds of table 4.6-1. The peaks observed mean that one (or more) stars were detected very far from the SATU detection point and, in this case, the stars were lost during the centering phase (see section 3.2 for stars lost in centering).

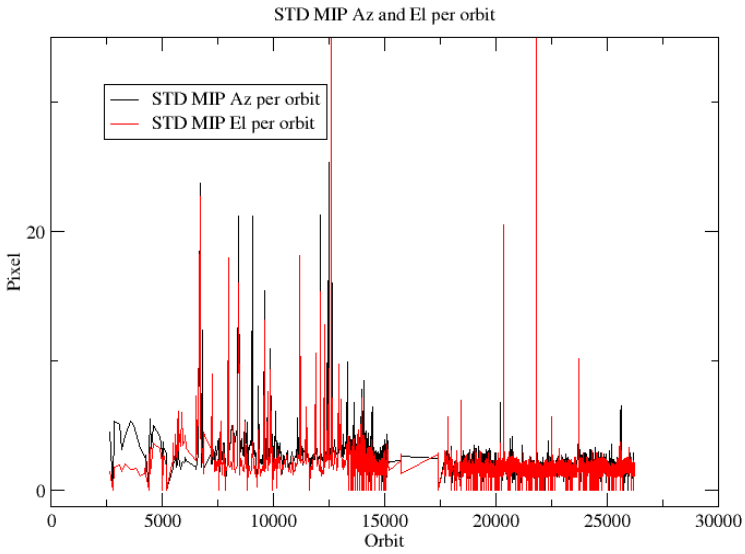

Figure 4.6-8: Standard deviation of MIP Azimuth and Elevation for some orbits since 1st September 2002 until end of reporting period (see table 4.6-1)

5 LEVEL 1 PRODUCT QUALITY MONITORING

5.1 Processor Configuration

5.1.1 VERSION

About 14% of near real time GOM_TRA_1P products have been received by the DPQC team for routine quality control and long term trend quality monitoring. The current level 1-processor software version for the operational ground segment is GOMOS/5.00 since 8th August 2006 (see table 5.1-1). The product specification is PO-RS-MDA-GS2009_10_3I. This processor has been cleared for level 1 data release, with a disclaimer for known artefacts (http://envisat.esa.int/dataproducts/availability/disclaimers) that are currently being resolved and will be implemented in following releases of the processor (http://envisat.esa.int/dataproducts/availability).

Table 5.1-1: PDS level 1b product version and main modifications implemented

Date	Version	Description of changes
08-AUG-2006	Level 1b version 5.00 at PDHS-E, PDHS-K	Algorithm baseline level 1b DPM 6.3 • Correction of FP unfolding algorithm • Background correction of SPB in full dark limb • Modification of the computation of the incidence angle • Correction of the flat-field correction equations • Star spectrum location on CCD modified for SPB • Provide SFA and SATU angles in degrees • Elevation angle dependency of the reflectivity LUT added in the algorithms • Ratio upper/star signal added (FLAGUC) • Add Dark Charge used for dark charge correction (per band) • Flag for illumination condition (PCDillum) • Minimum sample value for which the cosmic rays detection processing is applied (Crmin) is a function of gain index • Logic for computation of the flags attached to the reference star spectrum (Flref) modified • Add the computation of the sun direction in the inertial geocentric frame to be written in the level 1b and limb products. • Spectrometer effective sampling time added Change in configuration at the time of switch over: o Use of new reflectivity LUT (GOM_CAL_AX) o New wavelength assignment for SPA1, A2, B1 (GOM_CAL_AX) o Location of star spectrum projection on the CCD arrays (GOM_CAL_AX) o Spatial PSF of SPB modified (GOM_INS_AX) o Some universal constants (GOM_PR1_AX)
23-JUL-2006	Level 1b version 5.00 at LRAC	
23-MAR-2004	Level 1b version 4.02 at PDHS-E and PDHS-K	Algorithm baseline level 1b DPM 6.0 • Adding a new calibration parameters (these values are hard coded at the moment) • Removal of redundancy chain from code • Modifications in the processing to apply new configuration and calibration parameter • New algorithm to determine between dark, twilight and bright limb and to handle data accordingly • Added handling of source packages with invalid packet header • Added enumerations for all configuration flags
31-MAY-2003	Level 1b version 4.00 at PDHS-E and PDHS-K	Algorithm baseline level 1b DPM 5.4: • Modulation correction step added after the cosmic rays detection processing • Inversion of the non-linearity and offset corrections • Modification of the computation of the estimated background signal measured by the photometers: use the spectrometer radiometric sensitivity curve and the photometer transfer function. • Use of the dark charge map at orbit level computed from the DSA (dark sky area) if any in the level 0

		product • Implementation of a new unfolding algorithm for the photometer samples
21-NOV-2002	Level 1b version 3.61 at PDHS-E and PDHS-K	Algorithm baseline DPM 5.3: • Review of some default values • New definition of one PCD flag (atmosphere) • Temporal interpolation of ECMWF data

Users are also supplied with 2002 - 4th July 2006 data sets reprocessed by the last prototype processor GOPR_6.0c_6.0f developed and operated by ACRI. See table 5.1-2 for prototype level 1b versions and modifications. The current GOMOS operational ground segment version GOMOS/5.00 is line with the prototype version used for this second reprocessing.

Table 5.1-2: GOPR level 1b product version and main modifications implemented

Date	Version	Description of changes
22-JUL-2005	GOPR_6.0c	Level 1b: • Correction of FP unfolding algorithm • Background correction of SPB in full dark limb • Modification of the computation of the incidence angle • Correction of the flat-field correction equations • Star spectrum location on CCD modified for SPB Configuration for second reprocessing: o Use of new reflectivity LUT o New wavelength assignment for SPA1, A2, B1 o Spatial PSF of SPB modified
17-MAR-2004	GOPR 6.0a	• Provide SFA and SATU angles in degrees • Elevation angle dependency of the reflectivity LUT added in the algorithms • Ratio upper/star signal added (FLAGUC) • Add Dark Charge used for dark charge correction (per band) • Flag for illumination condition (PCDillum) • Minimum sample value for which the cosmic rays detection processing is applied (Crmin) is a function of gain index • Logic for computation of the flags attached to the reference star spectrum (Flref) modified • Add the computation of the sun direction in the inertial geocentric frame to be written in the level 1b and limb products. • Spectrometer effective sampling time added
25-JUL-2003	GOPR 5.4f	• The demodulation process is applied only in full dark limb and twilight limb conditions.
17-JUL-2003	GOPR 5.4e	• Sun zenith angle is computed in the geolocation process. The occultation is now classified into (0) full dark limb condition, (1) bright limb condition and (2) twilight limb condition. • No background correction applied in full dark limb condition. The location of the image of the star spectrum on the CCD array is no more aligned with the CCD lines.
02-JUL2003	GOPR 5.4d	• The maximum number of measurements is set to 509 (instead of 510) in the GOPR prototype.

17-MAR-2003	GOPR 5.4c	• Modification of the CAL ADFs (update of the limb radiometric LUT). The products are affected only if the limb spectra are converted into physical units • Modifications to allow compatibility with ACRI computational cluster (no modifications of the results) • Modification of the logic to handle dark charge map refresh at orbit level (DSA data is now directly processed by the level 1b processor if available in the level 0 product). No impact on the results
21-FEB-2003	GOPR 5.4b	• DC map values are rounded when written in the level 1b product • Modification of the CAL ADFs (update of the wavelength assignment of SPB1 and SPB2) • Modify the computation of flag_mod in the modulation correction routine
17-JAN-2003	GOPR 5.4a	• use the start and stop dates of the occultation when calling the CFI Interpol instead of start and stop dates of the level 0 product • modify the ECMWF filename information in the SPH of the level 1b and limb products

5.1.2 AUXILIARY DATA FILES (ADF)

The ADF's files in tables 5.1-3, 5.1-4, 5.1-5, 5.1-6 and 5.1-7 have been disseminated to the PDS during the whole mission. Note that the files outlined in yellow are the set of auxiliary files used during the reporting period. For every type of file, the validity runs from the start validity time until the start validity time of the following one, but if an ADF file has been disseminated after the start validity time, it is obvious that it will be used by the PDHS-E and PDHS-K PDS only after the dissemination time (this happens the majority of the time). Just like the other ADF's, the calibration auxiliary file (GOM_CAL_AX) has been updated several times in the past (table 5.1-7) but the difference is that now it is updated in a weekly basis with only new DC maps, and that is why the files used during November 2006 are reported in a separate table (table 5.1-8) that changes from report to report.

Table 5.1-3: Table of historic GOM_PR1_AX files used by PDS for level 1b products generation. The GOM_PR1_AX is a file containing the configuration parameters used for processing from level 0 to level 1b products

Used by PDS for Level 1b products generation in period	GOM_PR1_AX (GOMOS processing level 1b configuration file)
01-MAR-2002 → 29-MAR-2002	**GOM_PR1_AXVIEC20020121_165314_20020101_000000_20200101_000000** • Pre-launch configuration
30-MAR-2002 → 14-NOV-2002	**GOM_PR1_AXVIEC20020329_115921_20020324_200000_20100101_000000** • Changed num_grid_upper, thr_conv and max_iter in the atmospheric GADS
Not used	**GOM_PR1_AXVIEC20020729_083756_20020301_000000_20100101_000000** • Cosmic Ray mode + threshold • DC correction based on maps • Non-linearity correction disabled
Not used	**GOM_PR1_AXVIEC20021112_170331_20020301_000000_20100101_000000** • Central background estimation by linear interpolation + associated thresholds

15-NOV-2002 → 26-MAR-2003	**GOM_PR1_AXVIEC20021114_153119_20020324_000000_20100101_000000** • Same content as GOM_PR1_AXVIEC20021112_170331_20020301_000000_20100101_000000 but validity start updated so as to supersede according to the PDS file selection rules GOM_PR1_AXVIEC20020329_115921_20020324_200000_20100101_000000
27-MAR-2003 → 19-MAR-2004	**GOM_PR1_AXVIEC20030326_085805_20020324_200000_20100101_000000** • Same content as GOM_PR1_AXVIEC20021112_170331_20020301_000000_20100101_000000 but validity start updated so as to supersede according to the PDS file selection rules GOM_PR1_AXVIEC20020329_115921_20020324_200000_20100101_000000
20-MAR-2004 → 22-MAR-2004	**GOM_PR1_AXVIEC20040319_134932_20020324_200000_20100101_000000** • Ray tracing parameter changed: convergence criteria set to 0.1 microrad
23-MAR-2004 → 01-APR-2004 *Notes*: • This file was constructed from GOM_PR1_AXVIEC20030326_085805_20020324_200000_20100101_000000 (so without the ray tracing parameter changed) • This file was used by the GOMOS/4.02 processors before the IECF dissemination. The dissemination was done on 25th March 2004	**GOM_PR1_AXVIEC20040316_144850_20020324_200000_20100101_000000** GOM_PR1 ADF for version GOMOS/4.02, changes: • The central band estimation mode • Atmosphere thickness • Altitude discretisation
02-APR-2004 → 07-AUG-2006	**GOM_PR1_AXVIEC20040401_083133_20020324_200000_20100101_000000** • Ray tracing parameter changed: convergence criteria set to 0.1 microrad
08-AUG-2006 Used at the time of switching over GOMOS/5.00	**GOM_PR1_AXNIEC20050627_151042_20020301_000000_20100101_000000** • Change of some universal constants

Table 5.1-4: Table of historic GOM_INS_AX files used by PDS for level 1b products generation. The GOM_INS_AX is a file containing the characteristics of the instrument and it is used for processing from level 0 to level 1b products and from level 1b to level 2 products

Used by PDS for Level 1b products generation in period	GOM_INS_AX (GOMOS instrument characteristics file)
01-MAR-2002 → 29-JUL-2002	**GOM_INS_AXVIEC20020121_165107_20020101_000000_20200101_000000** • Pre-launch configuration
30-JUL-2002 → 12-NOV-2002	**GOM_INS_AXVIEC20020729_083625_20020301_000000_20100101_000000** • Factors for the conversion of the SFA angles from SFM axes to GOMOS axes
13-NOV-2002 → 16-JUL-2003	**GOM_INS_AXVIEC20021112_170146_20020301_000000_20100101_000000** • No more invalid spectral range
Not used	**GOM_INS_AXVIEC20030716_080112_20030711_120000_20100101_000000** • New value for SFM elevation zero offset for redundant chain: 10004

17-JUL-2003 → 07-AUG-2006	**GOM_INS_AXVIEC20030716_105425_20030716_120000_20100101_000000** • Bias induct azimuth redundant value set to -0.0084 rad (-0.4813 deg)
08-AUG-2006 Used at the time of switching over GOMOS/5.00	**GOM_INS_AXNIEC20050627_150713_20030716_120000_20100101_000000** • The spatial PSF of SPB

Table 5.1-5: Table of historic GOM_CAT_AX files used by PDS for level 1b products generation. The GOM_CAT_AX is a file holding the star catalogue used for processing from level 0 to level 1b products

Used by PDS for Level 1b products generation in period	GOM_CAT_AX (GOMOS Stat Catalogue file)
01-MAR-2002	**GOM_CAT_AXVIEC20020121_161009_20020101_000000_20200101_000000** • Pre-launch configuration

Table 5.1-6: Table of historic GOM_STS_AX files used by PDS for level 1b products generation. The GOM_STS_AX is a file containing star spectra used for processing from level 0 to level 1b products

Used by PDS for Level 1b products generation in period	GOM_STS_AX (GOMOS Star Spectra file)
01-MAR-2002 → 07-AUG-2006	**GOM_STS_AXVIEC20020121_165822_20020101_000000_20200101_000000** • Pre-launch configuration
08-AUG-2006 Used at the time of switching over GOMOS/5.00	**GOM_STS_AXNIEC20040308_103538_20020101_160000_20100101_000000** • Wavelength assignment GADS has been suppressed from the product • Wavelength assignment vector has been added to the star spectrum

Table 5.1-7: Table of historic GOM_CAL_AX files used by PDS for level 1b products generation. The GOM_CAL_AX is a file containing the calibration parameters used for processing from level 0 to level 1b products

Used by PDS for Level 1b products generation in period	GOM_CAL_AX (GOMOS Calibration file)
01-MAR-2002 → 29-JUL-2002	**GOM_CAL_AXVIEC20020121_164808_20020101_000000_20200101_000000** • Pre-launch configuration
Not used	**GOM_CAL_AXVIEC20020121_142519_20020101_000000_20200101_000000** • Pre-launch configuration
30-JUL-2002 → 12-NOV-2002	**GOM_CAL_AXVIEC20020729_082426_20020717_193500_20100101_000000** • Band setting information • Wavelength assignment • Spectral dispersion LUT • ADC offset for Spectrometers • PRNU maps • Thermistor coding LUT • DC maps
Not used	**GOM_CAL_AXVIEC20021112_165603_20020914_000000_20100101_000000** • Band setting information • DC maps • PRNU maps • Wavelength assignment • Spectral dispersion LUT • Radiometric sensitivity LUT (star and limb) • SP-FP intercalibration LUT • Vignetting LUT

	• Reflectivity LUT • ADC offset
13-NOV-2002 → 30-JAN-2003	**GOM_CAL_AXVIEC20021112_165948_20021019_000000_20100101_000000** • Only DC maps updated
31-JAN-2003 → 11-APR-2003	**GOM_CAL_AXVIEC20030130_133032_20030101_000000_20100101_000000** • Only DC maps updated (using DSA of orbit 04541)
12-APR-2003 → 02-JUN-2003	**GOM_CAL_AXVIEC20030411_065739_20030407_000000_20100101_000000** • Modification of the radiometric sensitivity curve for the limb spectra. Note that the modification of this LUT has no impact on the GOMOS processing. The LUT is just copied into the level 1b limb product for user conversion purpose. • Updated DC map only (using DSA of orbit 05762).
03-JUN-2003: from this date onwards, mainly updates to DC maps are done. Every month, the table of new GOM_CAL files with **only** DC maps updated is provided (table 5.1-8). Eventual changes to this file not corresponding only to DC maps updates will be reported in this table.	**GOM_CAL_AXVIEC20030602_094748_20030531_000000_20100101_000000** • Updated DC maps only (using DSA of orbit 06530)
13-FEB-2004 → 23-FEB-2004	**GOM_CAL_AXVIEC20040212_103916_20040209_000000_20100101_000000** • Update of the reflectivity LUT • Updated DC maps (Orbit 10194, date 11-FEB-2004)
08-AUG-2006 Used at the time of switching over GOMOS/5.00	**GOM_CAL_AXNIEC20050704_110915_20050125_224800_20100101_000000** • Reflectivity LUT updated • Location of the star spectrum projection on the CCD arrays • Wavelength assignment of the spectra updated • The spatial LSF of SPB updated • Updated DC maps (orbit 15200, date 25 JAN 2005)

Table 5.1-8: Calibration ADF for reporting period. These files are updated (only with DC maps) in a 8-10 days basis

Used by PDS for Level 1b products generation in period	GOM_CAL_AX (GOMOS Calibration file)
10-FEB-2007 → 20-FEB-2007	**GOM_CAL_AXVIEC20070209_111315_20070208_000000_20100101_000000** (orbit 26017 , date 08 FEB 2007)
21-FEB-2007 → 06-MAR-2007	**GOM_CAL_AXVIEC20070221_092417_20070220_000000_20100101_000000** (orbit 26219 , date 20 FEB 2007)

5.2 Quality Flags Monitoring

In this section, the results of monitoring some Product Quality information stored in level 1b products that did not have a fatal error (MPH error flag not set) are discussed. The products with fatal errors were around 8,0% of the products received during the reporting month for the quality monitoring.

On the one hand, for every product we have information of the **number of measurements** where a given problem was detected (i.e. number of invalid measurements, number of measurements containing saturated samples, number of measurements with demodulation flag set…). On the other hand, there are **flags** that

indicate problems within the product (i.e. flag set to one if the reference spectrum was computed from DB, flag set to zero if SATU data were not used…).

For the information on the number of measurements a plot of percentages with respect to time is provided in fig. 5.2-1. The most relevant part of this information is also plotted in a world map as a function of ENVISAT position: % of cosmic ray hits per profile, % of datation errors per profile, % of star falling outside the central band per profile and % of saturation errors per profile (fig.5-2.2).

It can be seen from fig. 5.2-1 that the cosmic rays hits occurred several times for the 95% of the measurements of the products. Looking at fig. 5.2-2 it can be clearly observed that this high percentage occurred when the satellite crossed the South Atlantic Anomaly (SAA) zone. Also the percentage of saturation errors per profile shows an increase over the SAA zone.

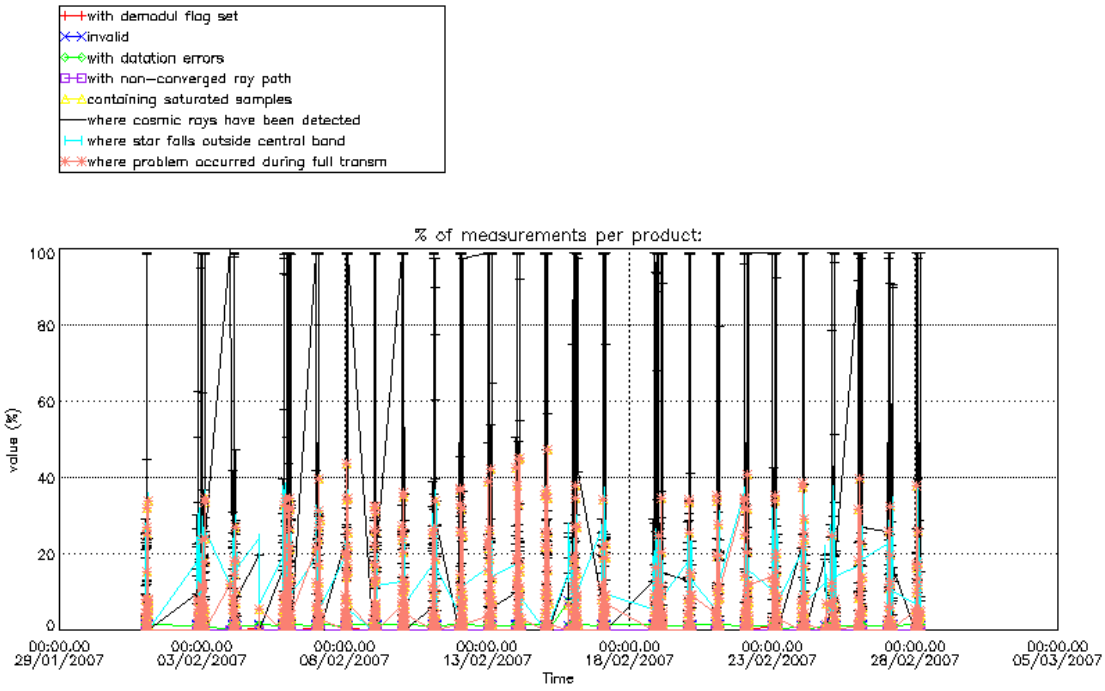

Figure 5.2-1: Level 1b product quality monitoring with respect to time

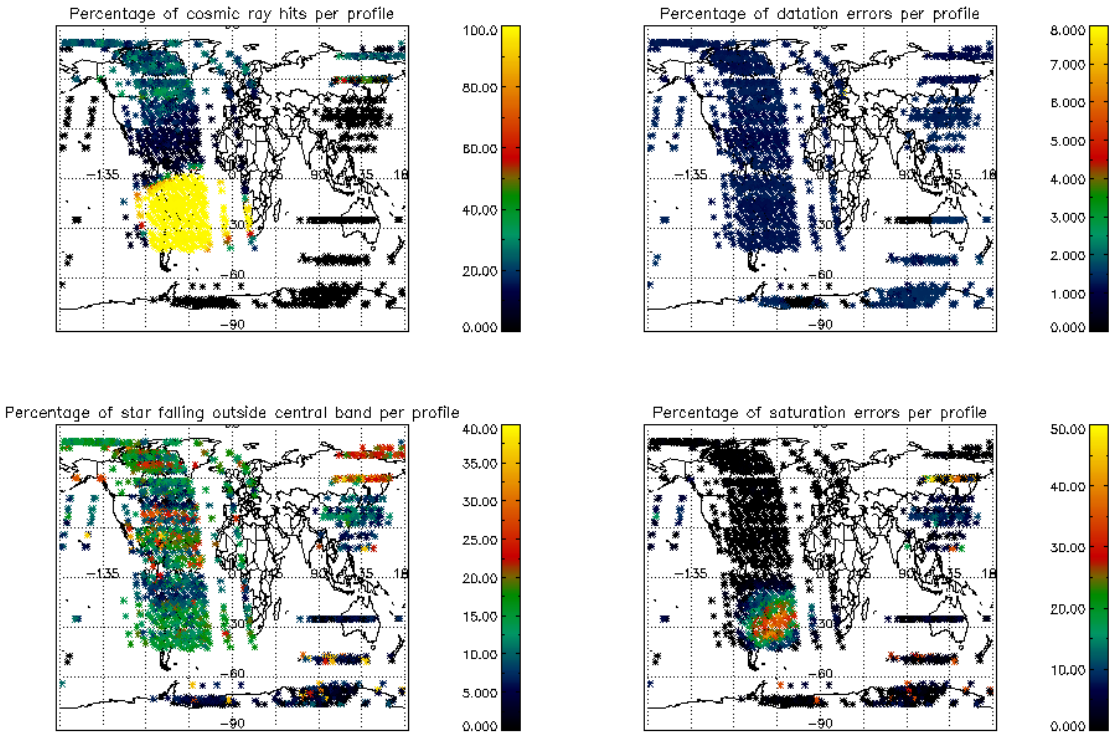

Figure 5.2-2: Level 1b product quality monitoring with respect to geolocation of ENVISAT

Another observation from fig. 5.2-1 is that for many products, 20-25% of the measurements have the star signal falling outside the central band. In fig. 5.2-2 it is observed that this percentage occurred mainly during twilight/dark conditions while in bright conditions the percentage is around 10% (fig.5.2-2). This is because during the night the stars are lost deeper within the atmosphere and the turbulence phenomena becomes more important, producing the star to be less 'focused' on the spectrometers central band.

The other values (% of invalid measurements per product, % of measurements per product with datation errors…) are quite low.

The flag information is given in table 5.2-1. The percentage of the products that have at least one measurement with demodulation flag set is also reported.

Table 5.2-1: Percentage of products during the reporting period with:

At least one measurement with demodulation flag set:	29.8 %
Reference spectrum computed from DB:	0.0 %
Reference spectrum with small number of measurements:	0.0 %
SATU data not used:	0.0 %

5.2.1 QUALITY FLAGS MONITORING (EXTRACTED FROM LEVEL 2 PRODUCTS)

In this section, the Product Quality information coming from the level 1 processing that is also stored in the level 2 products is plotted. Only products that did not have a fatal error (MPH error flag not set) are considered. The purpose of using the level 2 data is simply that the percentage of level 2 products arriving to the DPQC team for the quality monitoring is much higher. For the reporting month, 77% of the archived products have been received. The plots are very similar to fig. 5.2-1 and 5.2-2 (demodulation flag information is not included) but separating ascending from descending passes. Since new version of the processor (GOMOS/5.00) there is no correspondence between illumination condition and latitude range when separating the passages (ascending and descending). Now, in the geolocation process, the sun zenith angle is computed and the occultation is then flagged accordingly (dark, bright, twilight, straylight, twilight+straylight). You can see in fig. 5.2-3 the location of the occultations and their limb for the reporting month.

Fig. 5.2-4 and 5.2-5 present some quality information as a function of the time whereas in fig. 5.2-6 and 5.2-7 the plot is respect to the satellite position at the beginning of the occultations.

In ascending (fig. 5.2-4) the percentage of measurements “where a problem occurred during the full transmission” per product is around 2% while for the descending passes (fig. 5.2-5) is between 10-45%. In particular around the middle of the month we observed a significant increase of this value. This is due to the saturation that occurs mainly in bright limb. In dark limb the saturation occurs over the SAA zone but it is quite low elsewhere. From fig. 5.2-4 and 5.2-5 you can see also that there are a variable percentage of the measurements that have the star signal falling outside the central band. This is because in dark the stars are lost deeper within the atmosphere and the turbulence phenomena become more important, resulting in the star being less ‘focused’ on the spectrometers central band.

In ascending (fig. 5.2-6) the SAA is perfectly localized by the high percentage of cosmic ray hits per product (upper left panel). It is not the same if we look at fig. 5.2-7, because in descending most of the occultations in that world region are in bright limb conditions and the cosmic rays detection processing is not activated.

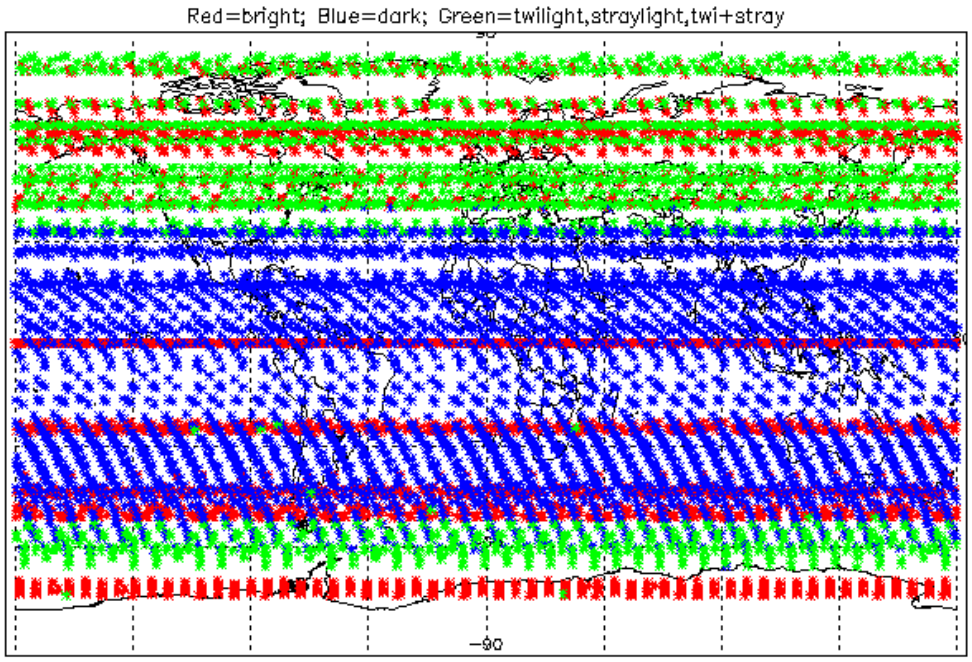

Figure 5.2-3: Position of the occultations based on illumination conditions

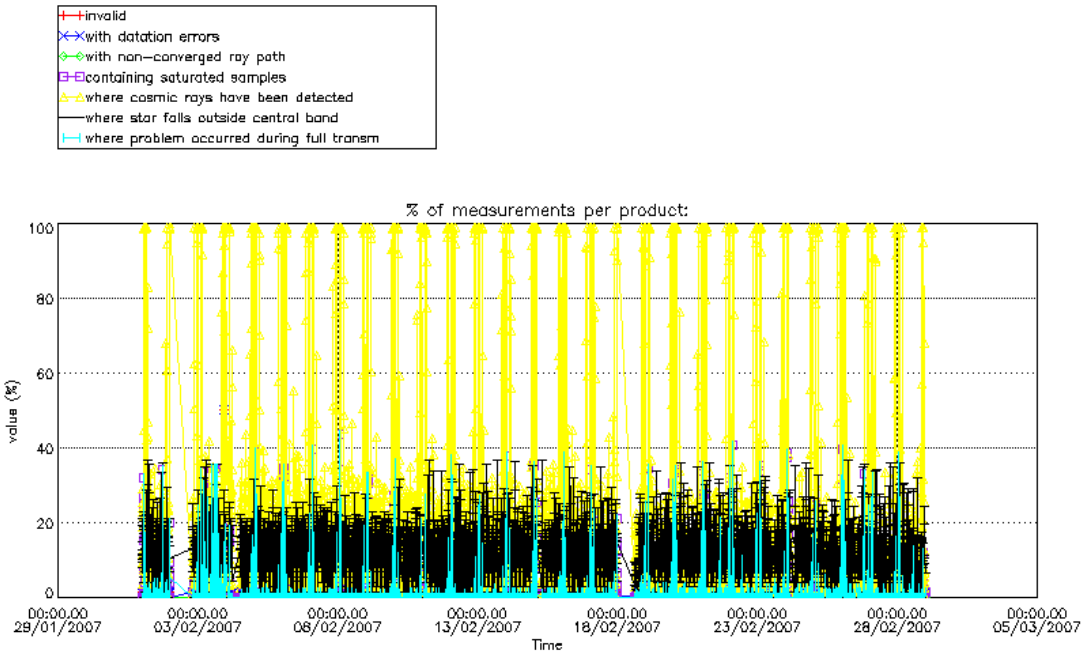

Figure 5.2-4: Level 1b product quality monitoring with respect to time ASCENDING ENVISAT passes

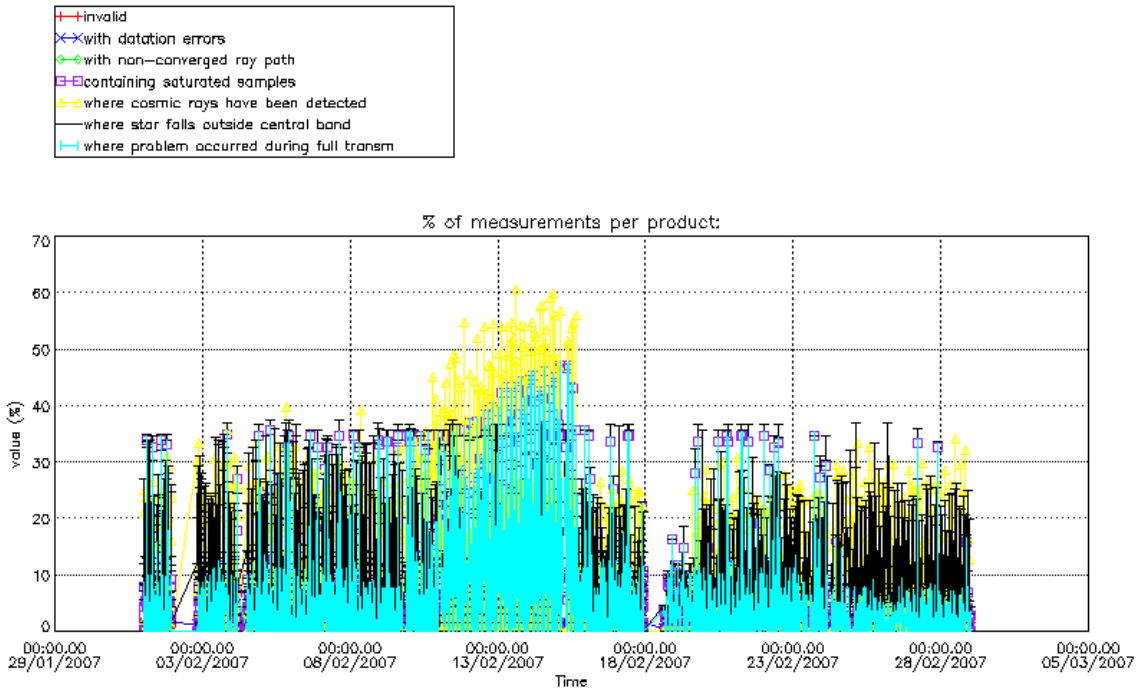

Figure 5.2-5: Level 1b product quality monitoring with respect to time DESCENDING ENVISAT passes

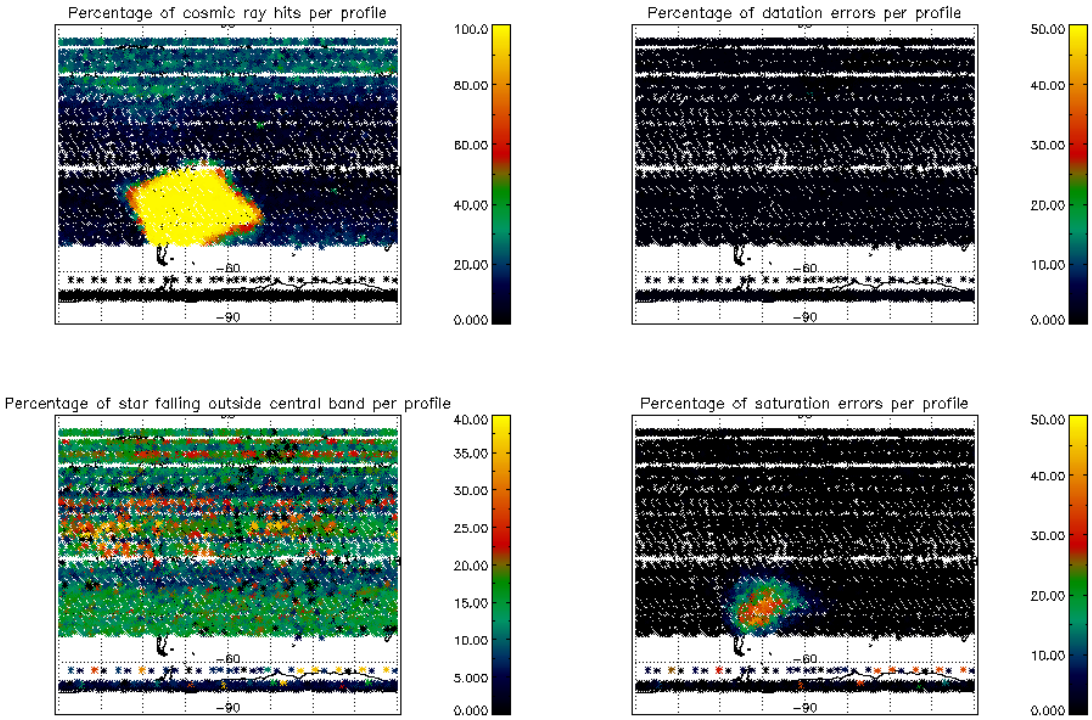

Figure 5.2-6: Level 1b product quality monitoring with respect to geo-location for ASCENDING ENVISAT passes

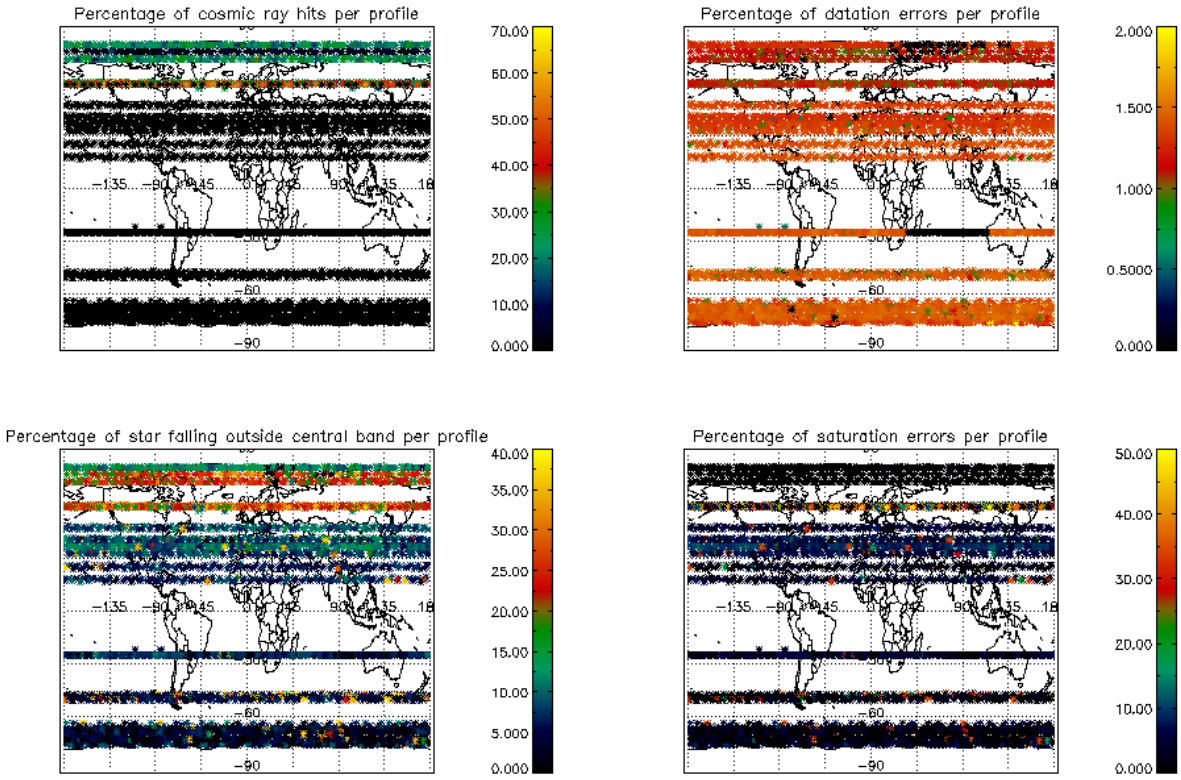

Figure 5.2-7: Level 1b product quality monitoring with respect to geo-location for DESCENDING ENVISAT passes

5.3 Spectral Performance

In previous spectral calibration exercises the results exceeded the warning value which is 0.07 nm (fig. 5.3-1). Since 8th August 2006, in parallel to the switch to GOMOS/5.00, a new set of ADFs is in use, and the wavelength shifts are again within the threshold. This set of ADF was used also for the second reprocessing (2002-4th July 2006), so good wavelength characterization has been used for the second reprocessing.

The values reported in the plot of fig. 5.3-1 are, for every star ID (1, 2, 9, 18, 25), the spectral shift on SPA2 CCD for which a maximum correlation has been found between the reference spectrum and the one of the occultation. During the last wavelength calibration analysis performed using some occultations of star id 1, 2 and 9 measured during August, the spectral shifts were again within the threshold.

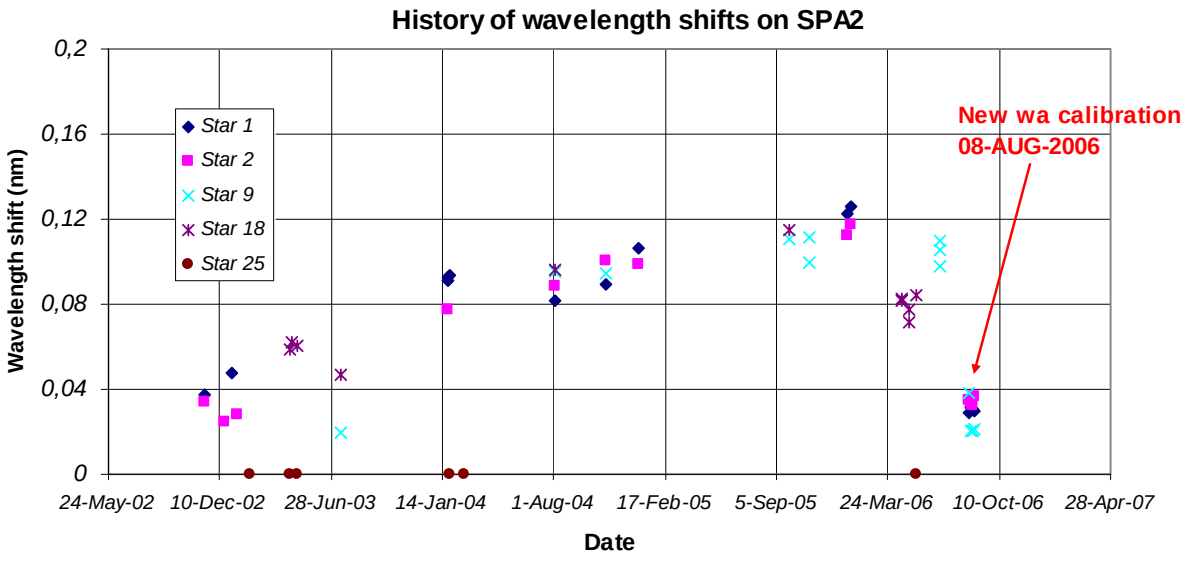

Figure 5.3-1: Wavelength shifts on SPA2 since 12th November 2002 calculated using different stars

5.4 Radiometric Performance

5.4.1 RADIOMETRIC SENSITIVITY

The monitoring performed consists of the calculation of the radiometric sensitivity of each CCD by computing the ratio between parts of the reference spectrum using specific stars (fig. 5.4-1). The parts of the spectrum used are:

- UV: 250–300 nm
- Yellow: 500–550 nm
- Red: 640–690 nm
- Ir1: 761-770 nm
- Ir2: 935-944 nm

UV

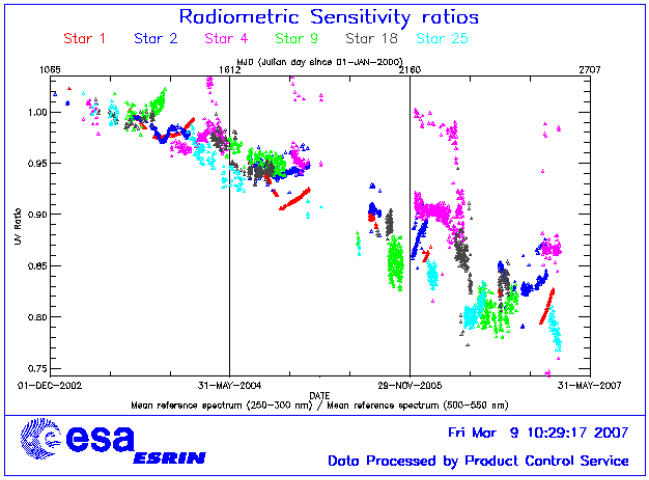

VIS

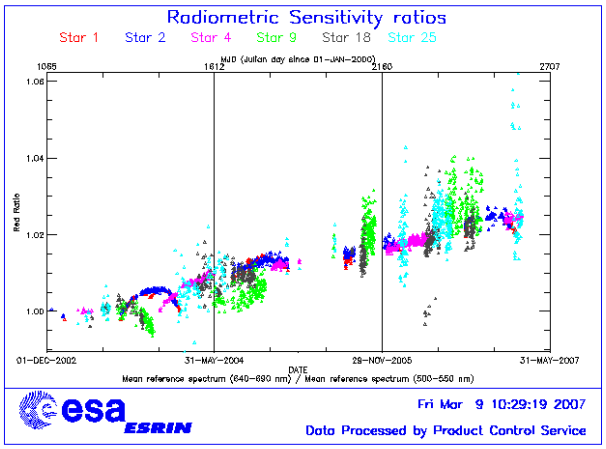

IR1

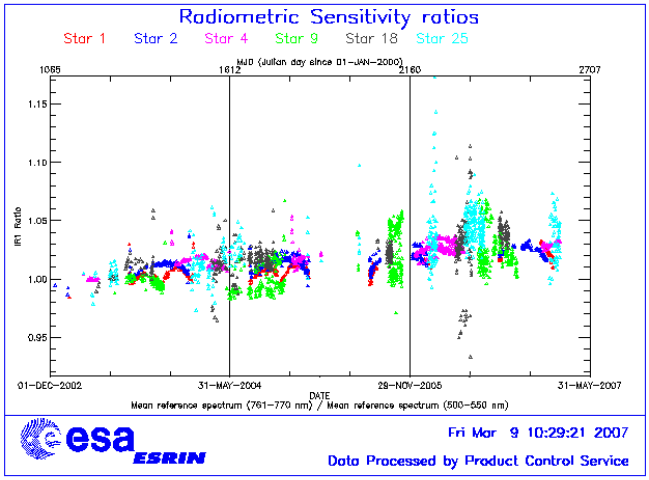

IR2

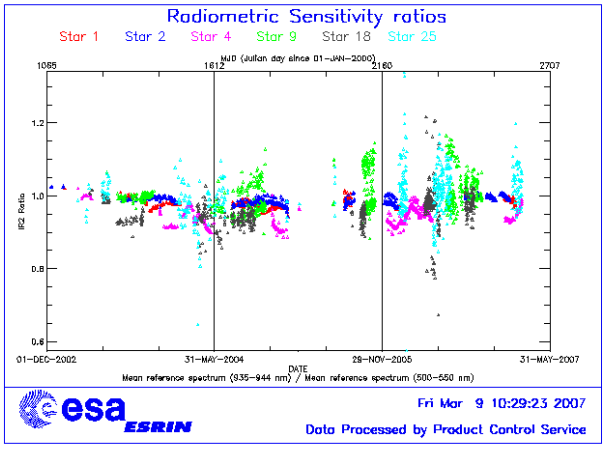

PH1

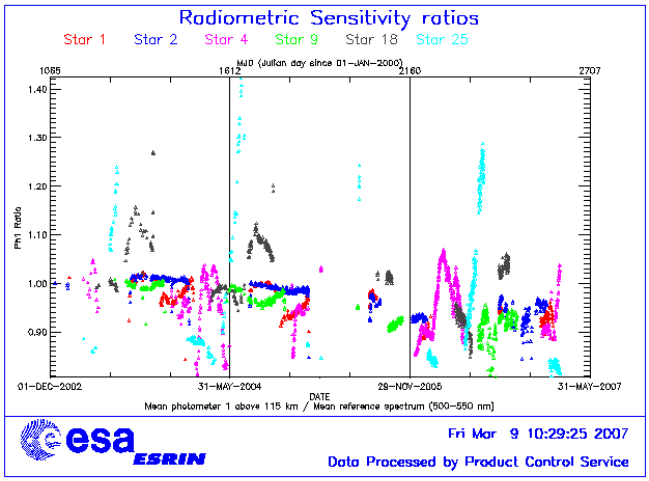

PH2

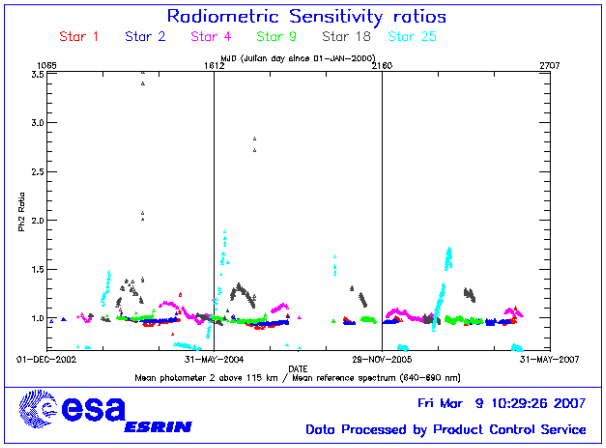

Figure 5.4-1: Radiometric sensitivity ratios since December 2002

For the spectrometers the ratios are with respect to the 'yellow' spectral range. For the photometers, the ratios are calculated by dividing the mean photometer signal above the atmosphere (115 km) by the 'yellow' spectral range (for PH1) or by the 'red' spectral range (for PH2).

The variation of the ratio should be within a given threshold which is set to 10% (see table 5.4-1 that corresponds to fig. 5.4-1). For every star, this variation is calculated as the difference between the maximum (or minimum) ratio, and the mean over the 15 first values (if there were not 15 values computed yet, all values would be used).

Table 5.4-1: Variation of RS for the different ratios (corresponds to fig. 5.4-1). Should be less than 10%

Star Id	% Variation of UV ratio	% Variation of Red ratio	% Variation of IR1 ratio	% Variation of IR2 ratio	% Variation of Ph1 ratio	% Variation of Ph2 ratio
1	4.47216	0.843367	0.421901	0.250543	8.55029	30.1656
2	1.11971	1.15509	0.625175	0.383392	8.42268	8.34067
4	0.645188	1.63999	1.52463	1.30163	8.08780	23.5227
9	16.4895	1.35384	0.799394	0.603875	11.1437	9.05862
18	3.17715	1.41829	1.63441	1.76815	14.7885	299.989
25	32.2603	1.96732	1.85261	1.35782	28.0870	147.396

For star 9 and 25 the UV ratio is greater than the threshold 10%. It is clear (fig. 5.4-1) that there is a global decrease of UV ratios for all the stars. This confirms the expected degradation suffered by the UV optics that is, anyway, very small considering also the small variation for the rest of the stars (table 5.4-1).

By looking at the photometers radiometric sensitivity ratios of fig. 5.4-1, it can be seen that every star has a variation that seems to be annual. The variation is significant for stars 25 and 18. After some investigations performed by the QWG that exclude an inaccurate reflectivity correction LUT, it seems that the PH1/2 radiometric sensitivity variations could come from the fact that the spectrometers and the photometers are not illuminated the same way when the straylight appears (seasonal effect).

5.4.2 PIXEL RESPONSE NON UNIFORMITY

No new PRNU calibration has been performed during the reporting period. This means that the PRNU maps inside the ADF remain as they are without any change for the moment.

5.5 Other Calibration Results

Future reports will address other calibration results, when available.

6 LEVEL 2 PRODUCT QUALITY MONITORING

6.1 Processor Configuration

6.1.1 VERSION

Level 2 products from the operational ground segment have been disseminated during the reporting period to the users. About 93% of GOM_NL__2P products have been received by the DPQC team for routine quality control and long term trend monitoring. The current level 2-processor software version for the operational ground segment is GOMOS/5.00 since 8th August 2006 (see table 6.1-1). The product specification is PO-RS-MDA-GS2009_10_3I. Users are also supplied with 2002 - 4th July 2006 data sets reprocessed by the last prototype processor GOPR_6.0c_6.0f (developed and operated by ACRI) which is in line with the current GOMOS operational ground segment version GOMOS/5.00

Table 6.1-1: PDS level 2 product version and main modifications implemented

Date	Version	Description of changes
08-AUG-2006	Level 2 version 5.00 at PDHS-E and PDHS-K	Algorithm baseline level 2 DPM 6.2: • The optimisation of the DOAS iterations • Negative column densities and local densities not flagged anymore • Suppress the setting of maximum error in case of negative local densities • Correction of HRTP discrepancies, and error estimates fixed • Rename Turbulence MDS into High Resolution Temperature MDS (HRTP) • Add vertical resolution per species in local densities MDS • Add Solar zenith angle at tangent point and at satellite level in geolocation ADS • Add "tangent point density from external model" in geolocation ADS • Suppress contribution of "tangent point density from external model" in "local air density from GOMOS atmospheric profile" in geolocation ADS Change in configuration at the time of the switch over: o 2nd order polynomial for aerosol o Air fixed to ECMWF (local density set to 0 in the L2 products) o Orphal cross-sections for O_3 o GOMOS cross-sections for other species o Covariance matrix terms linked to air set to 0 o Air and NO_2 additional errors set to 0
23-JUL-2006	Level 2 version 5.00 at FinCoPAC	
23-MAR-2003	Level 2 version 4.02 at PDHS-E and	Algorithm baseline level 2 DPM 5.5:

	PDHS-K	Section 3 • Add references to technical notes on Tikhonov regularization • Change High level breakdown of modules: SMO/PFG • Change parameter: NFS in l2 ADF • Change parameter σ_G in l2 ADF (Table 3.4.1.1-II) • Change content of Level 2/res products – GAP • Change time sampling discretisation • Add covariance matrix explanation Section 5 • Replace SMO by PFG VER-1/2: Depending on NFS, Apply either a Gaussian filter or a Tikhonov regularization to the vertical inversion matrix • Unit conversion applied on kernel matrix • Suppress VER-3 Section 6 • GOMOS Atmospheric Profile (GAP): not used in this version • Time sampling in equation (6.5.3.7-73)
31-MAY-2003	Level 2 version 4.00 at PDHS-E and PDHS-K	Algorithm baseline level 2 DPM 5.4: • Revision of some default values • Add a new parameter • Transmission model computation: suppress tests on valid pixels and species • Apply a Gaussian filter to the vertical inversion matrix • Very low signal values are substituted by threshold value
21-NOV-2002	Level 2 version 3.61 at PDHS-E and PDHS-K	Algorithm baseline level 2 DPM 5.3a: • Revision of some default values • Wording of test T11 • Dilution term computation of jend • Covariance computation scaling applied before and after

Table 6.1-2: GOPR level 2 product version and main modifications implemented

Date	Version	Description of changes
14-OCT-2005	GOPR_6.0f	• The optimisation of the DOAS iterations • Negative column densities and local densities not flagged anymore • Suppress the setting of maximum error in case of negative local densities • Correction of HRTP discrepancies, and error estimates fixed Configuration for second reprocessing: o 2nd order polynomial for aerosol o Air fixed to ECMWF (local density set to 0 in the L2 products)

		o Orphal cross-sections for O_3 o GOMOS cross-sections for other species o Covariance matrix terms linked to air set to 0 o Air and NO_2 additional errors set to 0
17-MAR-2004	GOPR 6.0a	• Rename Turbulence MDS into High Resolution Temperature MDS (HRTP) • Add vertical resolution per species in local densities MDS • Add Solar zenith angle at tangent point and at satellite level in geolocation ADS • Add "tangent point density from external model" in geolocation ADS • Suppress contribution of "tangent point density from external model" in "local air density from GOMOS atmospheric profile" in geolocation ADS
18-AUG-2003	GOPR 5.4d	• Tikhonov regularisation is implemented
18-MAR-2003	GOPR 5.4b	• Modification to implement the computation of Tmodel for spectrometer B (in version 5.4b, the Tmodel for SPB is still set to 1)
30-JAN-2003	GOPR 5.4a	• Modifications for ACRI internal use only. No impact on level 2 products.

6.1.2 AUXILIARY DATA FILES (ADF)

The ADF's files in table 6.1-3 and 6.1-4 are used by the PDS to process the data from level 1 to level 2. For every type of file, the validity runs from the start validity time until the start validity time of the following one, but if an ADF file has been disseminated after the start validity time, it is obvious that it will be used by the PDHS-E and PDHS-K PDS only after the dissemination time (this happens the majority of the time). Note that the files outlined in yellow are the set of auxiliary files used during the reporting period.

Table 6.1-3: Table of historic GOM_PR2_AX files used by PDS for level 2 products generation. The GOM_PR2_AX is a file containing the configuration parameters used for processing from level 1b to level 2 products

Used by PDS for Level 2 products generation in period	GOM_PR2_AX (GOMOS Processing level 2 configuration file)
01-MAR-2002 → 29-JUL-2002	**GOM_PR2_AXVIEC20020121_165624_20020101_000000_20200101_000000** • Pre-launch configuration
30-JUL-2002 → 02-SEP-2002	**GOM_PR2_AXVIEC20020729_083851_20020301_000000_20100101_000000** • Maximum value of chi2 before a warning flag is raised (set to 5) • Maximum number of iterations for the main loop (set to 1)
03-SEP-2002 → 12-NOV-2003	**GOM_PR2_AXVIEC20020902_151029_20020301_000000_20100101_000000** • Maximum value of chi2 before a warning flag is raised (set to 100)
13-NOV-2003 → 22-MAR-2004	**GOM_PR2_AXVIEC20021112_170458_20020301_000000_20100101_000000** • Smoothing mode • Hanning filter • Number of iterations • Spectral windows to suppress the O2 absorption in the high spectral range of SPA2
23-MAR-2004 *Note*: this file was used by the GOMOS/4.02 processors before the IECF dissemination. The	**GOM_PR2_AXVIEC20040316_145613_20020301_000000_20100101_000000** • Pressure at the top of the atmosphere • Number of GOMOS sources data (used in GAP)

dissemination was done on 25th March 2004	• Activation flag for GOMOS sources data (GAP) • Smoothing mode (after the spectral inversion) • Atmosphere thickness
08-AUG-2006 Used at the time of switching over GOMOS/5.00	GOM_PR2_AXNIEC20051021_081111_20020301_000000_20100101_000000 • Several level 2 processing configuration parameters

Table 6.1-4: Table of historic GOM_CRS_AX files used by PDS for level 2 products generation. The GOM_CRS_AX is a file containing the cross sections used for processing from level 1b to level 2 products

Used by PDS for Level 2 products generation in period	GOM_CRS_AX (GOMOS Cross Sections file)
01-MAR-2002 → 08-MAR-2002	GOM_CRS_AXVIEC20020121_164026_20020101_000000_20200101_000000 • Pre-launch configuration
09-MAR-2003 → 29-JUL-2002	GOM_CRS_AXVIEC20020308_185417_20020101_000000_20200101_000000 • Corrected NUM_DSD in MPH - was 14 and is now 19 - and corrected spare DSD format by replacing last spare by carriage returns in file GOM_CRS_AXVIEC20020121_164026_20020101_000000_20200101_000000
30-JUL-2002 → 25-MAR-2004	GOM_CRS_AXVIEC20020729_082931_20020301_000000_20100101_000000 • O3 cross-sections summary description (SPA) • NO3 cross-sections summary description • O2 transmissions summary description • H2O transmissions summary description • O3 cross sections (SPA)
26-MAR-2004 *Note*: the file was disseminated on 27 Jan 2004 but could not be used by PDS until version GOMOS/4.02 was in operation	GOM_CRS_AXVIEC20040127_150241_20020301_000000_20100101_000000 • Update of the O2 and H2O transmissions (S.A input) • Extension by continuity of the O3 cross-section for SPB
08-AUG-2006 Used at the time of switching over GOMOS/5.00	GOM_CRS_AXNIEC20051021_080452_20020301_000000_20100101_000000 • Updated O_3 cross-sections

6.1.3 RE-PROCESSING STATUS

The improvement of the GOMOS processing chain is a continuous on-going activity, not only for the processing algorithm but also for the instrument characterization data. In order to provide the best quality products to the users and due to the normal delay between algorithm specification and implementation in the operational PDS, it has been decided to reprocess the GOMOS data using the GOPR prototype.

The second reprocessing activity covering years 2002-2006 (until 4th July 2006) using the prototype GOPR_6.0c_6.0f is completed. All reprocessed data can be retrieved via web query from http://www.enviport.org/gomos/index.jsp. FTP access to bulk reprocessing results (one tar file of GOMOS products per day) is allowed from the D-PAC: ftp://gomo2usr@ftp-ops.de.envisat.esa.int. See more details and latest status on http://www.enviport.org/boards/board_gomos.htm

6.2 Quality Flags Monitoring

In this section, some information contained in the Quality Summary data set of the level 2 products of November 2006 is shown. In particular, the percentage of flagged points per profile for the local species O_3, H_2O, NO_2 and NO_3 is depicted. Only products in dark limb illumination conditions and without fatal errors (error flag in the MPH set to "0") are used.

The flagging strategy for GOMOS version GOMOS/5.00 foresees that a profile point is flagged when:

- The local density is greater than a given maximum value
- The line density is not valid. And it occurs when:
  - The acquisition from level 1b is not valid
  - There is no acquisition used for reference star spectrum
  - The line density is greater than a given maximum value

  Only for species: air, aerosol, O_3, NO_2, NO_3, OClO
  - No convergence after a given number of LMA iterations
  - χ^2 out of LMA is bigger than χ^2
  - Failure of inversion

  Only for species: O_2, H_2O
  - Spectro B only: no convergence
  - Spectro B only: data not available
  - Spectro B only: covariance not available

There are points mainly between -80° and +30° latitude (fig. 6.2-1) because in this period of the year full dark illumination condition occultations (only those products have been used for these plots) are geo-located on that region. In summer, full dark illumination data are mainly in the Southern Hemisphere while in winter it is the contrary: full dark illumination occultations are found mainly in the Northern Hemisphere.

Looking at fig. 6.2-1, the most evident characteristic that can be observed is the high percentage of flagged points per profile for some H_2O profiles. Users should be careful in using these data as the quality is only guaranteed for few stars. As a consequence of the new flagging strategy the percentage of flagged points per profile for O_3, NO_2 and NO_3 is around 10-15%. It can be seen also that there are latitudinal bands with almost the same color (same percentages) mainly for H_2O. This means that the percentages of flagged points per profile have a dependence on the stars that have been observed: a given star is always observed at the same latitude but at different longitude.

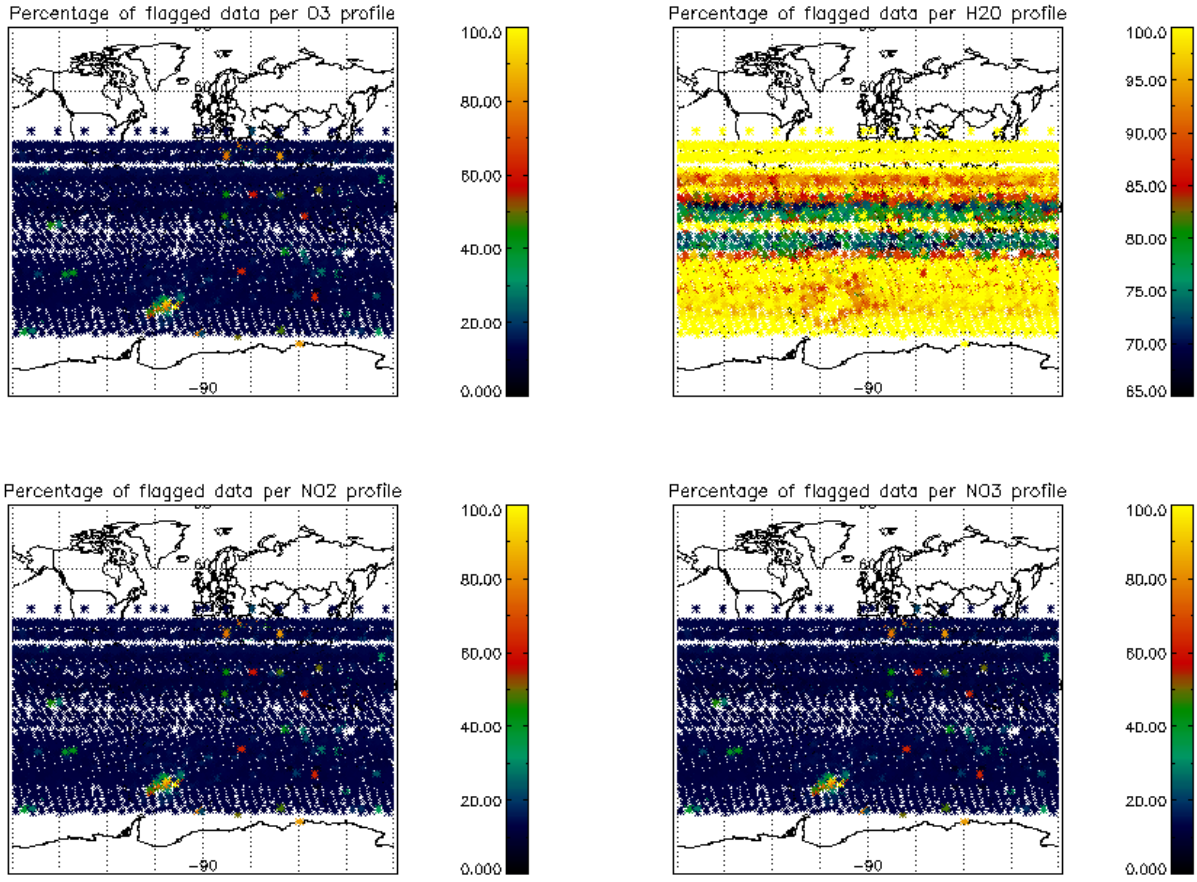

Figure 6.2-1: Percentage of flagged points per profile

6.3 Other Level 2 Performance Issues

The plot presented in fig. 6.3-1 is the average of the Ozone values during the reporting month in a grid of 0.5 degrees in latitude per 1 km in altitude. Only occultations in dark limb have been used. Even though there is a reduction on latitude coverage due to the restricted azimuth field of view of the instrument, still some known characteristics can be seen:

- O_3 concentrations show a decrease with latitude near 40 km altitude. In the lower latitudes O_3 is generated by photolysis of O_2
- In the middle stratosphere (25-30 km) O_3 is strongly influenced by transport effects. Strong meridional and zonal transport is visible in middle and higher latitudes
- The lower stratosphere shows an O_3 increase with latitude. Highest values can be found within higher latitude regions due to downward transport of rich air masses

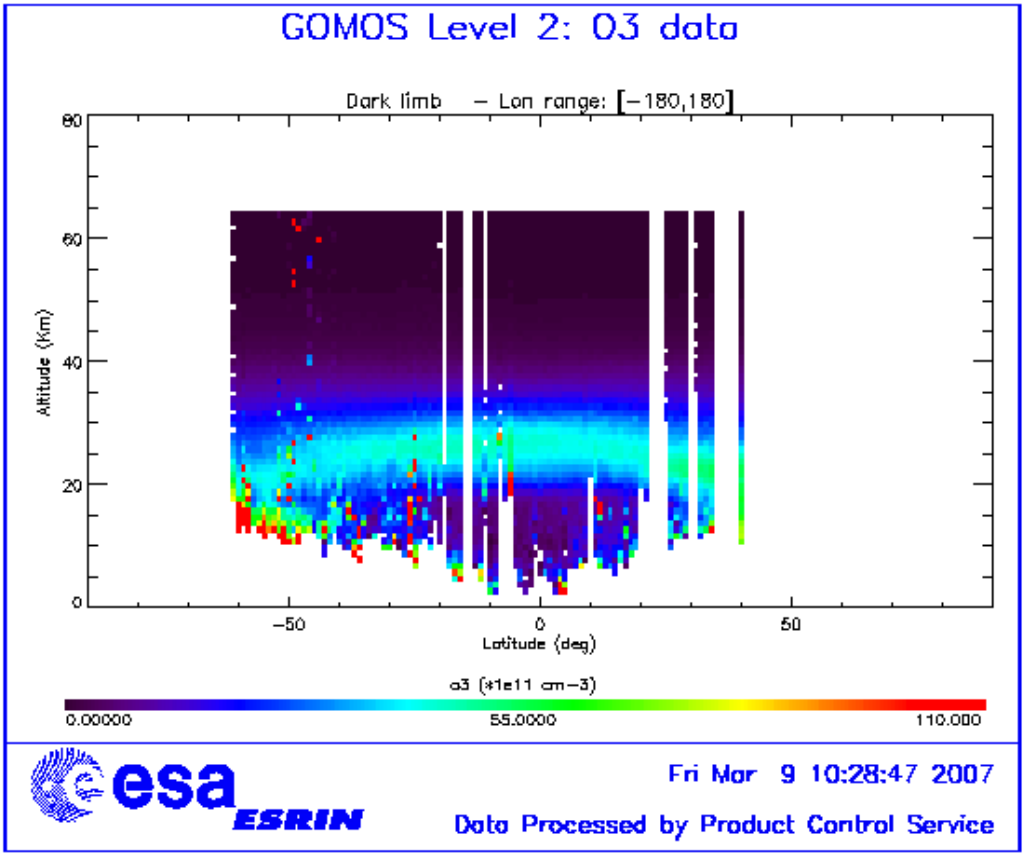

Figure 6.3-1: Average GOMOS O_3 profile during the reporting month: average in a grid of 0.5° latitude x 1 km altitude

7 VALIDATION ACTIVITIES AND RESULTS

7.1 GOMOS-ECMWF Comparisons

The full ECMWF validation report is available at the following address:
http://earth.esa.int/pcs/envisat/calval_res/2007/ecmwf_gomos_monthly_200702_all.pdf
A summary of the report is reported below.

7.1.1 KEY POINTS FOR FEBRUARY 2007

The quality of NRT GOMOS temperature data was generally found stable during February 2007 and consistent with that for January 2007.
Good agreement was found between GOMOS and ECMWF temperatures. NRT GOMOS temperatures were lower than ECMWF temperatures in all the stratosphere and mesosphere.
The mean departures between GOMOS temperatures and ECMWF temperature analyses were less than -1% (about -2K) in all the stratosphere, up to 1hPa. Negative departures down to -2% (about -4K) were found, on

global average, in the mesosphere. The agreement between the data and the ECMWF first guess and analyses slightly deteriorated in the mesosphere at high latitudes in the SH, where the first guess temperature departures are on average -5 to -6%, corresponding to about -10K.
The global mean departures between GOMOS and ECMWF ozone profiles were still found very large, with +50% differences in places,in the upper stratosphere and mesosphere.
Large scatter of GOMOS ozone data was found at most latitudes, especially at high latitudes where a few outliers can still be found.
Scatter plots still showed unrealistically low GOMOS ozone values (0 DU) at some vertical levels in the upper troposphere and mesosphere, but they are no longer found in the stratosphere.
The quality of the water vapour retrievals is still quite poor. Unrealistically low GOMOS water vapour values (0 mg/m2) as well as very large first-guess departures (100%) were found at most vertical levels.
The monitoring statistics for February 2007 were produced with the operational ECMWF model, CY31R2.

7.1.2 QUALITY AND AMOUNT OF RECEIVED DATA

Data coverage and amount of received data during February 2007 are shown in figures 1 and 2 in the temperature, ozone and water vapour reports. Overall, more than 5000 (good) observations were available for ozone and more than 7000 for temperature, with the largest number of observations available in the mesosphere and upper stratosphere, and only a fraction of them were available in the lower stratosphere (see figure 3 in the attached temperature and ozone reports). For what concerning the water vapour, about 1200 (good) observations were available in the period under consideration, with the largest number in the stratosphere (see figure 3 in the attached water vapour report).

7.1.3 GOMOS TEMPERATURE DATA

The quality of GOMOS NRT temperature was found generally stable during February 2007 and consistent with January.
The profile plots (temperature report: Figures 3-8) showed that, in the global average, the averaged GOMOS temperature is lower than that from the ECMWF temperature analyses over most of the stratosphere and mesosphere, with departures of about -1% (about -2K) up to 1hPa, and within 0 and -2% (about -4K) higher up. The NRT GOMOS temperatures were found to be lower than the ECMWF temperature analyses at most latitudinal bands and at all levels (temperature report: Figures 3-8). A slight deterioration in the agreement between GOMOS temperature observations and the ECMWF first guess and analyses was found in the mesosphere at high latitudes in the SH, where both the first guess and analysis departures increases up to -5 to 6% (about -10K) compared with the -4% departure found in January.
As seen in January, the scatter plots (temperature report: Figures 9-16) still show a relatively small scatter of the observations in the southern hemisphere, but larger at mid and high latitudes in the northern hemisphere, where the data oscillate within 10K around the mean, that leads to large first-guess departures at these latitudes. This large scatter in the northern hemisphere can be seen in most of the mesosphere, while the scatter plots in the stratosphere exihibit similar features of those presented in January, with a variability of the first-guess departures within 4K.
The Hovmoeller plots and the time series of GOMOS temperatures and departures at several levels are shown in Figures 17, 18, 21-24 of the temperature report, respectively. With the exception of the mesospheric high latitudes, where relatively large departures were seen between NRT temperature retrievals and the ECMWF temperature analyses (up to 10K difference), the quality of the data is generally stable, and

in a reasonably good agreement with the ECMWF analyzed ozone fields (first-guess departures being typically within 5K).

7.1.4 GOMOS OZONE DATA

The quality of GOMOS NRT ozone was generally found stable in February and consistent with that in January.
The profile plots (ozone report: Figures 3-8) showed that in the global average, the first-guess departures are within -2 and +15% in most of the stratosphere. Larger departures can still be found in both the mesosphere and troposphere, where, in particular, the first-guess biases can be larger than +50%. When averaged over latitudinal bands, the first-guess departures are generally within -2 and +20% in most of the stratosphere and lower mesosphere from 30S to 60N. Larger departures can be seen at high latitudes (especially in the SH) and at mid latitudes in the SH.
However, the standard deviations of the departures and of the GOMOS ozone data were still found larger than 50% at most vertical levels, indicative of large noise in the data. This is confirmed by the scatter plots (ozone report: Figures 9-16), which show large scatter in the GOMOS ozone data at all vertical levels and at all latitudes, that leads to large scatter in the first guess departures. The plots also show unrealistically low (around 0 DU) GOMOS ozone values in the mesosphere and upper stratosphere. These low values are no longer found at most levels in the low and mid stratosphere, that is an indication of improvements in the quality of the ozone retrievals. Still outliers can be seen at high latitudes in both hemispheres, that cause large first-guess departures at most vertical levels.
The timeseries of GOMOS ozone and departures at several levels and the Hovmoeller plots are shown in figures 17-20, and 21-22 of the ozone report, respectively. Both the timeseries and the Hovmoeller plots show some improvements in the agreement between NRT GOMOS ozone retrievals and the ECMWF ozone analyses, as found above.

7.1.5 WATER VAPOUR DATA

The quality of the water vapour data is generally poor at all vertical levels and latitudinal bands. As shown by most of the plots, there were several levels and latitudes for which no water vapour information was available.
The profile plots (water vapour report: Figures 3-5) showed that in the global average, the first-guess departures are larger than +100% at all vertical levels. When averaged over latitudinal bands, the agreement is not much better than that found in the global mean. The standard deviations of the departures and of the GOMOS ozone data were also large (much larger than 100%) at all vertical levels, indicative of very large noise in the data.
This is confirmed by the scatter plots (water vapour report: Figures 6-11), which show large scatter in the GOMOS water vapour data at all vertical levels and at all latitudes, that leads to large scatter in the first guess departures. The plots also show unrealistically low (around 0 mg/m2) GOMOS water vapour values at most vertical levels. Outliers can be seen at most latitudes in both hemispheres, that cause large first-guess departures at most vertical levels.
The Hovmoeller plots and the time series of GOMOS water vapour and departures at several levels are shown in Figures 13, and 15-16 of the water vapour report, respectively. Both the timeseries and the Hovmoeller plots show large differences between NRT GOMOS ozone retrievals and the ECMWF water vapour analyses.

It should be noted, however, that the monitoring statistics for water vapour was obtained from a very small number of observations, which was not probably statistically significant.

7.1.6 REMARKS

This monitoring report was produced with the operational ECMWF model (CY31R2). Ozone layers from SBUV/2 on NOAA-16 and SCIAMACHY total column ozone data produced by KNMI were actively assimilated.
The results presented in this reports made use of all the observations available in the BUFR files.
All ozone values are in Dobson Units (DU), temperatures are in K, and water vapour partial columns are in mg/m2.

7.2 QWG contribution to the GOMOS monthly report (February 2007)

7.2.1 CHARACTERIZATION OF NOISY O_2 PROFILES

A non-negligible number of O_2 vertical profiles in the GOMOS Level2 products include some noisy and non-flagged values of O_2 local density. We present here results on the first attempt of characterization of the noisy profiles, which is the prerequisite for future quality improvement of those products. The Level2 products used here were processed with the GOPR version 6.0cf which has been used for the second reprocessing of GOMOS products. This version of the prototype corresponds to the IPF version 5.00, currently in operation.

A possible dependence on the star characteristics and/or on the latitude region has been visually investigated by plotting all vertical profiles measured from a same star during 2003 and by latitude region. This has been performed for several stars providing a large number of full dark measurements with a wide latitude coverage. We present here results for two specific stars S1 and S23.

Results for S1 are plotted on Figure 2.

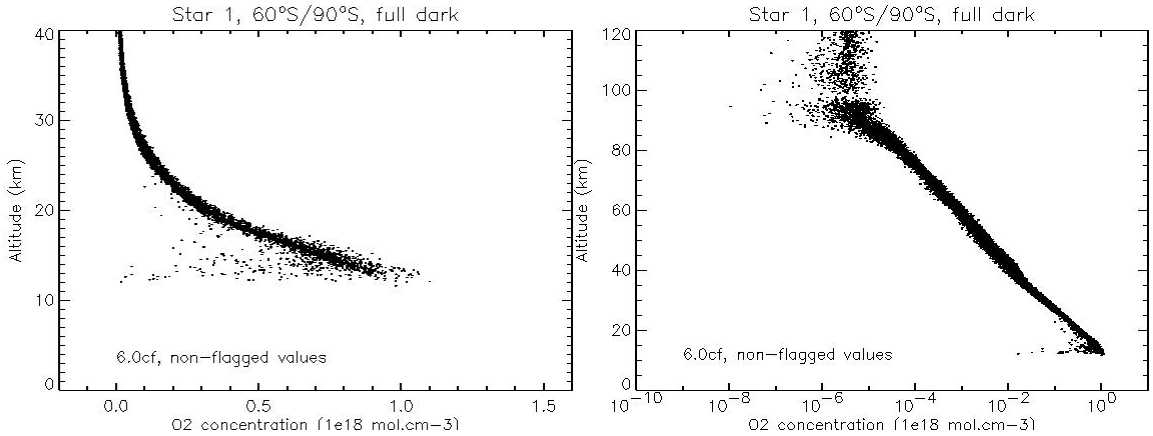

a) Results for S1 measurements at high latitudes in the Southern hemisphere.

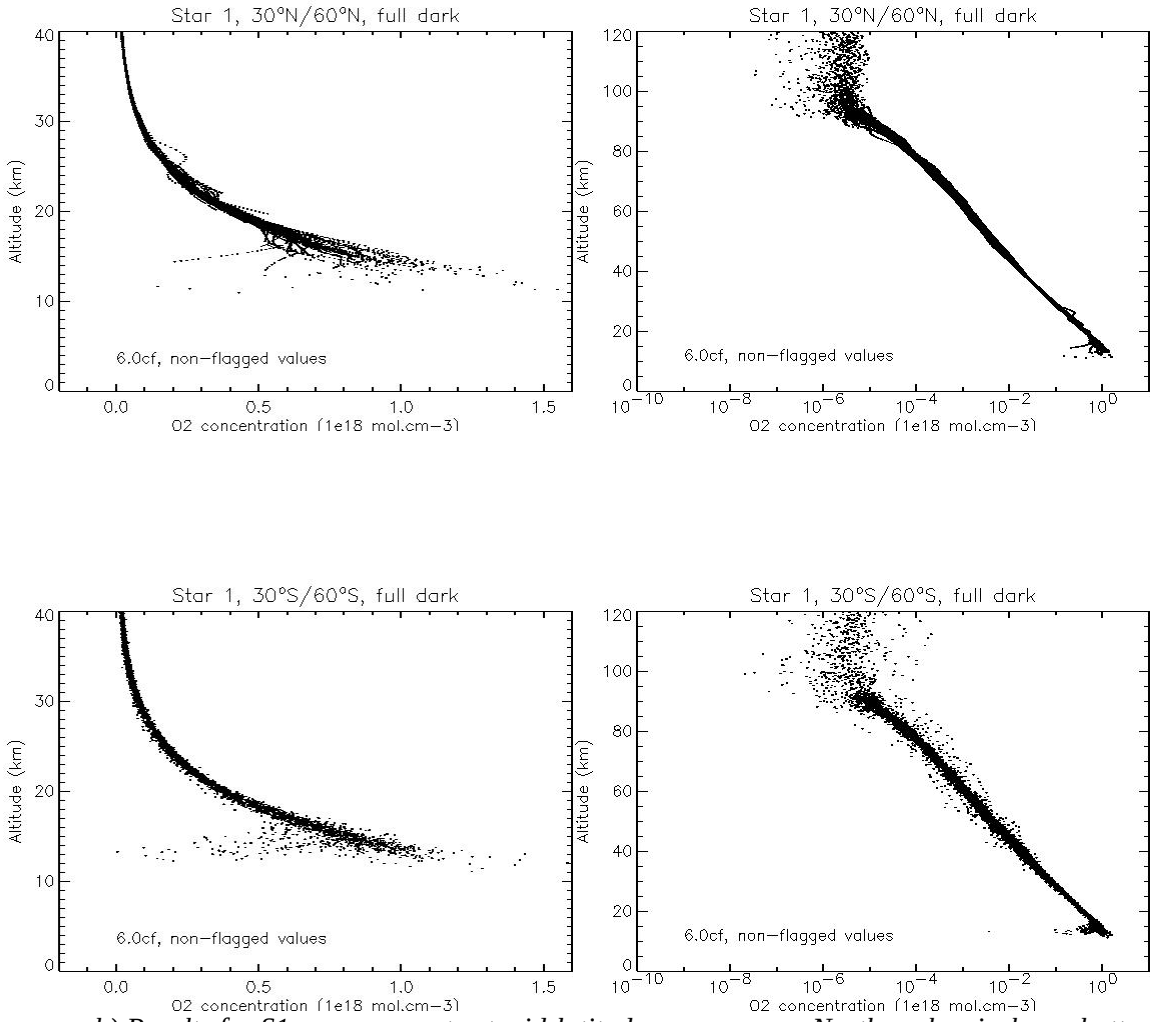

b) Results for S1 measurements at mid-latitudes; upper row: Northern hemisphere; bottom row: Southern hemisphere.

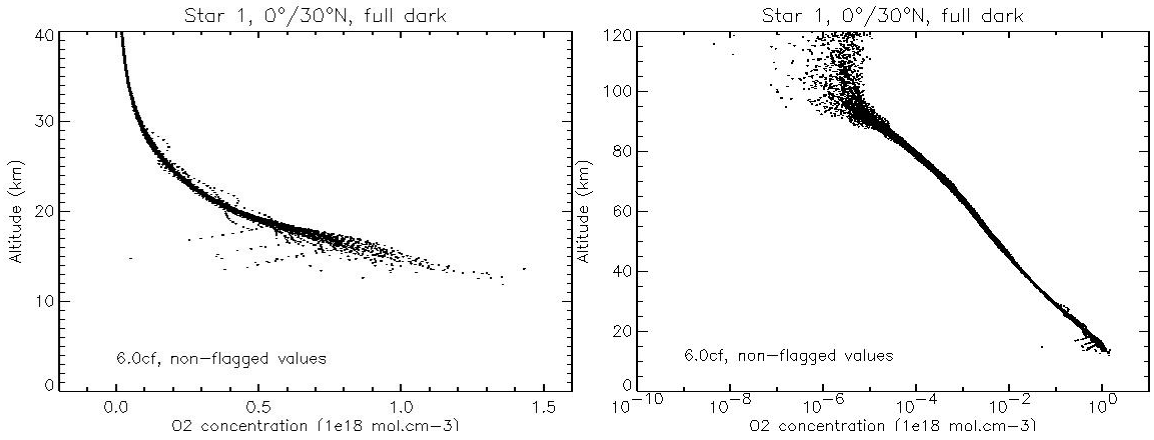

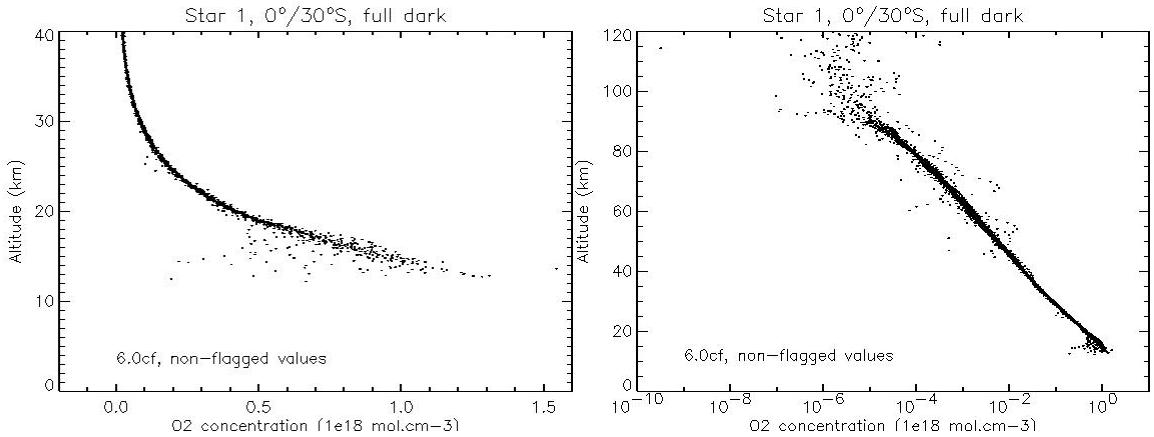

c) Results for S1 measurements at low latitudes; upper row: Northern hemisphere; bottom row: Southern hemisphere.

Figure 2: Vertical profiles of O_2 local density for all full dark measurements made in 2003 from S1, by latitude region. Left figures: altitude range between 0 and 40km, linear scale; right figures: altitude range between 0 and 120km, logarithmic scale.

For all latitude regions, some noisy values are present in the profiles; in the stratosphere, those outlier values are generally much lower than the average distribution. This is especially obvious in the Southern high latitude regions. Parts of profile with an unexpected shape are also present for some measurements in Northern mid-latitude regions, and in a smaller extent for some measurements in Northern low latitude regions.

In Northern mid-latitude regions, those profiles have been identified. The O_2 local density vs altitude for those profiles is presented on Figure 3, along with the median profile of the distribution for all S1 profiles of the latitude region. This confirms that for a same profile, several successive values are out of the average distribution.

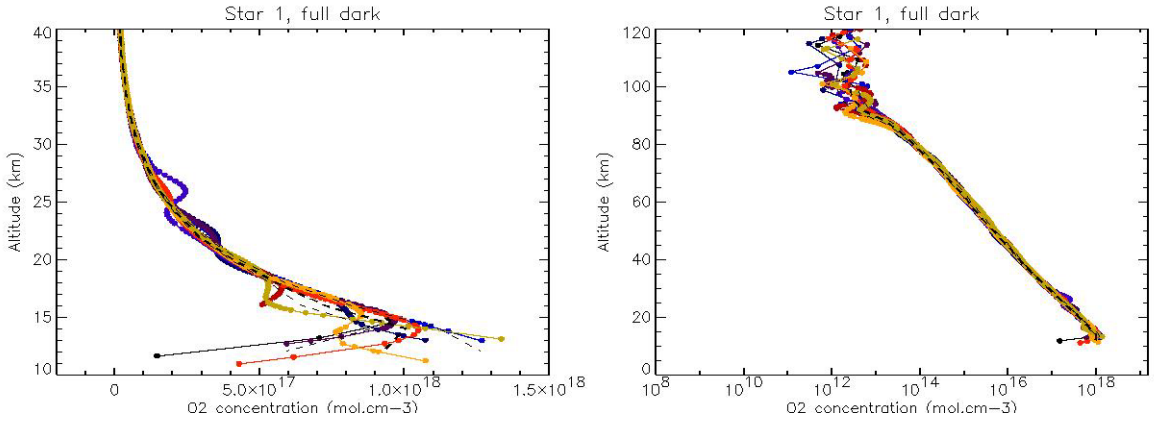

Figure 3: Vertical profiles of O_2 local density, for 22 identified measurements of S1 in the Northern mid-latitude regions presenting an unexpected shape; measurement dates are between 18/10/2003 and 21/10/2003; individual profiles are plotted with distinct colours; left figure: altitude range up to 40km, linear scale; right figure: altitude range up to 120km, logarithmic scale. The median profile and the dispersion of the complete distribution in the Northern mid-latitude regions are plotted with the dashed lines.

Results for S23 are plotted on Figure 4. Again, noisy O_2 values may be observed for all latitude regions. In Northern mid-latitudes, values much higher than the average distribution (values higher than 1.5 10^{18} molec cm-3 for some of them) are observed at lower altitude levels of the profiles.

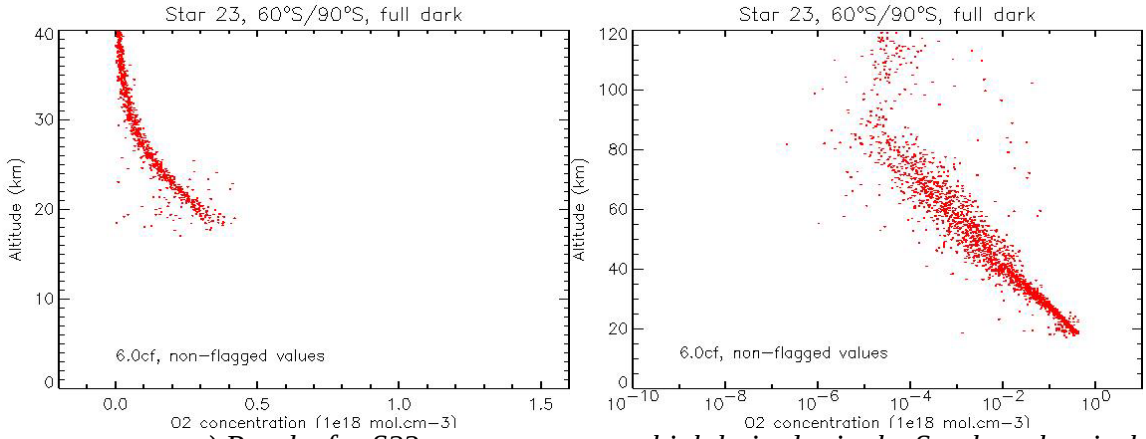

a) Results for S23 measurements at high latitudes in the Southern hemisphere.

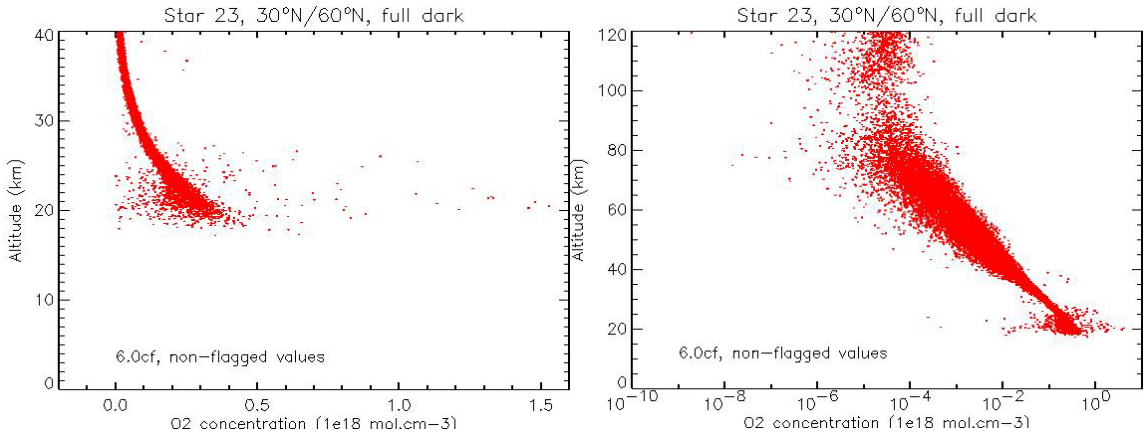

b) Results for S23 measurements at mid-latitudes in the Northern hemisphere.

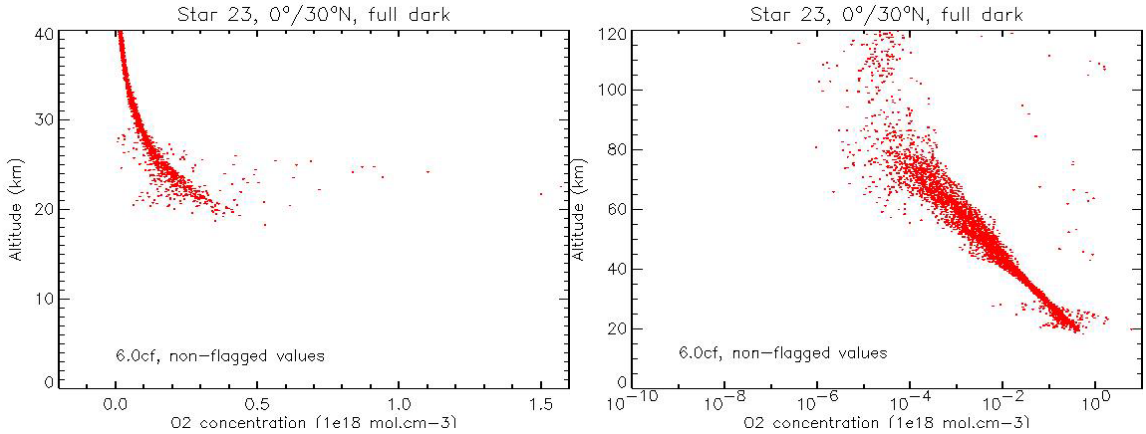

c) Results for S23 measurements at low latitudes in the Northern hemisphere.

Figure 4: Vertical profiles of O_2 local density for all full dark measurements made in 2003 from S23; left figures: altitude range up to 40km, linear scale; right figures: altitude range up to 120km, logarithmic scale.

The vertical profiles including values much higher than the average distribution in Northern mid-latitudes are detailed on **Figure 5**, along with the median profile of the distribution for all S23 profiles of the latitude region.

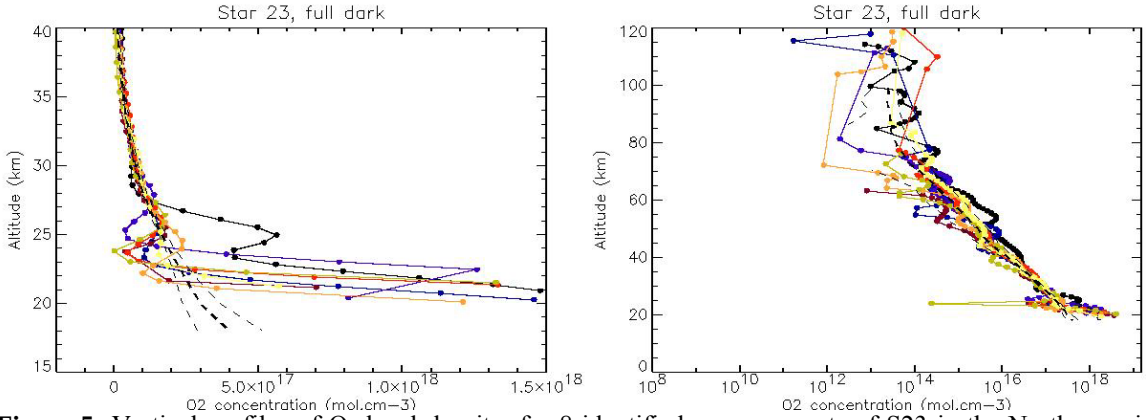

Figure 5: Vertical profiles of O_2 local density, for 8 identified measurements of S23 in the Northern mid-latitude regions with unexpected high values; measurement dates are between 10/11/2003 and 10/12/2003; individual profiles are plotted with distinct colours; left figures: altitude range up to 40km, linear scale; right figures: altitude range up to 120km, logarithmic scale. The median profile and the dispersion of the complete distribution in the Northern mid-latitude regions are plotted with the dashed lines.

As for S1, those results show that the overestimated values are not isolated outliers in the profile. Each profile may contain several successive overestimated values, usually in a quite large altitude range from a stratospheric level down to the bottom level of the profile. It is worth noting that those profiles also include some outliers in the mesosphere.

For the identified profiles with anomaly values, the comparison of O_2 local density values retrieved from GOMOS and inferred from ECMWF data is illustrated on Figure 6. For S1, between 10km and 40km, the comparison emphasizes the underestimation of O_2 density from GOMOS compared to ECMWF in a value range corresponding roughly to altitudes lower than 15km. For S23, it emphasizes the very high overestimation of O_2 density from GOMOS compared to ECMWF in a value range corresponding roughly to altitudes lower than 25km.

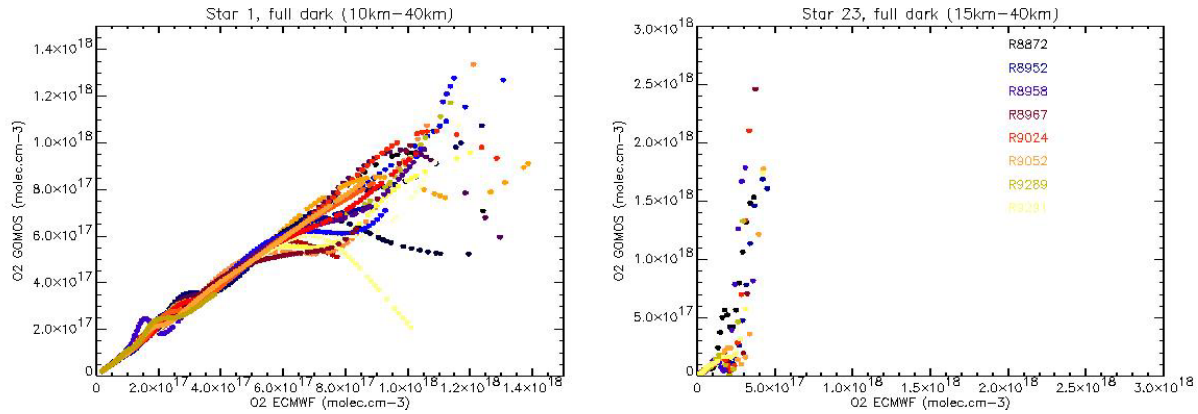

Figure 6: Values of O_2 local density from GOMOS vs values of O_2 local density inferred from ECMWF data; left figure: for S1 profiles plotted on Figure 3 and for altitude levels betwen 10km and 40km only; right figure: for S23 profiles plotted on Figure 5 and for altitude levels between 15km and 40km only.

Basing on these results, and on additional observations from S29, S30, S70, we conclude that noisy O_2 values are present in a large number of vertical profiles, in the stratosphere and in the mesosphere. There is no obvious dependence of the density of noisy values with the latitude region. There might be a larger number of noisy values for weaker stars than for brighter stars, but this would need to be further investigated.
In order to deepen this characterization study, the impact on the distribution of noisy O_2 values of selecting only non-flagged O_2 values corresponding to non-flagged O_3 values and to non-flagged aerosol values will be assessed. Further investigation will also be performed on the identified profiles showing anomaly values, for instance by carefully checking the density line values corresponding to noisy local density values.

7.3 GOMOS-Climatology comparisons

Results are presented when available.

7.4 GOMOS Assimilation

Results are presented when available.

7.5 Consistency Verification: GOMOS-GOMOS Inter-comparison

Results are presented when available.

7.6 Inter-Comparison with external data

Results are presented when available.